UNIVERSITÄT FÜR BODENKULTUR WIEN
University of Natural Resources
and Life Sciences, Vienna

Master Thesis

Soft sensor for determining oxygen consumption rate and viable cell count

submitted by

Martina Christine WINTER, B.Sc.

in the framework of the Master programme

Biotechnology

in partial fulfilment of the requirements for the academic degree

Diplom-Ingenieurin

Vienna, January 2023

Supervisor:

Priv. Doz. Dipl.-Ing. Peter Satzer, PhD

Co-supervisor:

Dipl.-Ing.in Lena Achleitner

Institute of Bioprocess Science and Engineering
Department of Biotechnology

Affidavit

I hereby declare that I have authored this master thesis independently, and that I have not used any assistance other than that which is permitted. The work contained herein is my own except where explicitly stated otherwise. All ideas taken in wording or in basic content from unpublished sources or from published literature are duly identified and cited, and the precise references included.

I further declare that this master thesis has not been submitted, in whole or in part, in the same or a similar form, to any other educational institution as part of the requirements for an academic degree.

I hereby confirm that I am familiar with the standards of Scientific Integrity and with the guidelines of Good Scientific Practice, and that this work fully complies with these standards and guidelines.

Vienna, 13th January 2022 Martina Christine WINTER (*manu propria*)

Acknowledgements

Dear reader,

I would first like to thank my thesis advisor Peter who offered this research topic to me. You allowed this paper to be my own work, but steered me in the right direction whenever I was in doubt. I am grateful for the space you gave me for acquiring programming skills and work self-reliantly. With all failures I encountered on the way, your realistic but also positive views encouraged me to a more confident mindset.

I would also like to thank my co-supervisor and dear friend Lena for your experience in fermentation processes and being there for all upcoming questions. I appreciate everything I could learn from you, not only in the daily lab-life but also as first reader of this thesis. Your advice and principles were a personal gain.

Further I want to express thanks to all colleagues and members of the virus group for including me as part of the team. I really enjoyed working and participating in so many occasions and extraordinary events with you. I look forward to our paths crossing again in the future.

To my dear friends Sophie, Felix, Birgit, and Brigitte, I am thankful for meeting you early through our studies and being able to look back fondly on so many shared memories. Your open ears and moral support have motivated me to my best.

To my family and Stefan, thank you for being there in every opportunity I take. Your constant support means everything to me.

This is not a goodbye to BOKU, but a see-you-soon, as the next challenge is awaiting me.

I am looking forward to everything that follows.

List of contents

Abbreviations

App.	approximately
CHO	Chinese hamster ovary
CIP	Cleaning in place
CPP	Critical quality attributes
CPR	CO_2 production rate
DNA	Deoxyribonucleic acid
DO	Dissolved oxygen
DoE	Design of Experiments
e.g.	Exempli gratia
EMA	European medicine agency
FBS	Fetal bovine serum
FDA	U.S Food and Drug Administration
HEK	Human embryonic kidney
ICH	International Council for Harmonisation of Technical Requirements for Pharmaceuticals for Human Use
mAb	Monoclonal antibody
MIR	Mid-infrared
NIR	Near infrared
OTR	Oxygen transfer rate
OUR	Oxygen uptake rate
PAT	Process analytical technology
PTMs	Post-translational modifications
QbD	Quality by Design
QbT	Quality by Testing
QRM	Quality risk management
QTTP	Quality target product profile
RO-H_2O	Reverse osmosis water
rpm	Revolutions per minute
Tn	*Trichoplusia ni*
US	United states h2o
UTC	Temps universel coordonn/ Coordinated Universal Time
UTC	Coordinated universal time
VCC	Viable cell concentration

Abstract

Regulatory authorities in biopharmaceutical industry emphasize process design by process understanding but applicable tools for upstream processes are still missing. In recent years, soft sensors have been proposed as promising tools for the implementation of the Quality by Design (QbD) approach and Process Analytical Technology (PAT), which enable higher process understanding. In particular, the correlation between viable cell counting and oxygen consumption was investigated, but problems remained: either the process had to be modified for excluding CO_2 in pH control, or complex $k_L a$ models had to be set up for specific processes. In this thesis, a non-invasive soft sensor for simplified on-line cell counting based on dynamic oxygen uptake rate was developed to close the gap to QbD and PAT. The dynamic oxygen uptake rates were determined by automated and periodic interruptions of gas supply in DASGIP® bioreactor systems, realized by a custom Visual Basic script in the DASware® control software. With off-line cell counting, the two parameters were correlated based on linear regression and led to a robust model with a determination coefficient of 0.97 Avoiding oxygen starvation during periodic shutdown of the gas supply was achieved by dynamic gas flow reactivation at a certain minimum dissolved oxygen concentration. The soft sensor was established in CHO fed-batch processes and implemented in the exponential growth phase. Control studies showed no impact on cell growth by of the discontinuous gas supply and changing dissolved oxygen concentration. This soft sensor is the first to be presented that does not require any specialized additional equipment as the methodology relies solely on the direct measurement of oxygen consumed by the cells in the bioreactor, achieved by the developed script.

Kurzfassung

Die Aufsichtsbehörden der biopharmazeutischen Industrie fordern Prozessdesign durch Prozessverständnis, aber es fehlen immer noch geeignete Werkzeuge für Upstream-Prozesse. Soft Sensoren werden als vielversprechendes Instrument für die Umsetzung des Quality by Design (QbD) Ansatzes und der Process Analytical Technology (PAT) vorgeschlagen, um Prozessverständnis ermöglichen. Insbesondere wurde die Korrelation zwischen der viablen Zellzahl und dem Sauerstoffverbrauch untersucht, aber Probleme blieben bestehen: Entweder musste der Prozess modifiziert werden, um CO_2 bei der pH-Kontrolle auszuschließen, oder es mussten komplexe $k_L a$ Modelle für spezifische Prozesse erstellt werden. In dieser Arbeit wurde ein nicht-invasiver Soft-Sensor für vereinfachte on-line Zellzählung auf der Grundlage der dynamischen Sauerstoffaufnahmerate entwickelt, um die Lücke zu QbD und PAT zu schließen. Die dynamischen Sauerstoffaufnahmeraten wurden durch automatisierte und periodische Unterbrechungen der Gaszufuhr in DASGIP® Bioreaktorsystemen bestimmt, realisiert durch ein programmiertes Visual Basic Skript in der DASware® Steuerungssoftware. Mit off-line Zellzahlbestimmung wurden die beiden Parameter auf Basis einer linearen Regression korreliert und führten zu einem robusten Modell mit einem Bestimmtheitsmaß von 0,97. Eine Begrenzung des Sauerstoffmangels wurde durch Reaktivierung des Gasflusses bei einer bestimmten Mindestkonzentration an gelöstem Sauerstoff erreicht. Der Soft Sensor wurde in Fed-Batch Prozessen mit CHO-Zellen etabliert und in der exponentiellen Wachstumsphase eingesetzt. Kontrollstudien zeigten keine Auswirkungen auf das Zellwachstum durch den potenziellen Einfluss einer diskontinuierlichen Gaszufuhr und einer sich ändernden Sauerstoffkonzentration. Dieser Soft Sensor ist der erste, der keine spezielle Zusatzausrüstung benötigt, da sich die Methodik ausschließlich auf die direkte Messung des Sauerstoffverbrauchs durch das entwickelte Skript stützt.

1. Introduction

In the past decades a trend in biopharmaceutical industry is visible: While more substantial research and intensive investments in novel drug development is made, the number of annually approved drugs is stagnating[1]. Measured by each billion US dollars of research and development costs spent, the number of approved drugs has halved every 9 years since 1950, considering inflation[2]. Moreover, only 2 out of 10 drugs return their research and development costs[3]. Consequently, the overall development costs have increased drastically, whereas the research and development efficiency has severely declined[2,4–6].

The reinvestment of revenues from successful drugs in research is also threatened by the expiration of numerous patents which leads to revenue losses and accelerates a general price competition as more off-patent drugs and biosimilars enter the market[7,8]. Examining the situation in further detail, the average success rate of potential drugs in Phase I clinical trials is at 12% or lower, after years of preclinical screening and evaluation[9,10]. To reduce the financial burden and accelerate the market entry of drug candidates, the manufacturing processes are developed in parallel to the clinical trials as these are the bottleneck[9]. The challenges of long and cost-intensive development paths in biopharmaceutical industry have provoked a rethinking of previous process development and quality regulations[11].

In other processing and manufacturing areas, such as milling, drying, granulation and tableting, the implementation of advanced technologies based on deepened process understanding was already successful[12]. Process understanding offers higher flexibility by managing the variability of process parameters while quality attributes are still met[13]. And higher flexibility in the manufacturing process reduces batch failures, overall costs, decreases regulatory burden (e.g. less deviations) and justifies post approval changes[14]. Additionally, barriers for innovation in development, manufacturing and quality assurance by process understanding become smaller and opportunities for process optimization open[15,16]. The development of personalized therapies would profit from this development as well, as these are inherently more variable processes[13,17,18]. Similarly, the COVID-19 pandemic highlighted the importance of rapid pharmaceutical development and flexibility in the production[19–21].

Different approaches have been described and widely accepted and promoted in guidelines by regulatory entities of biopharmaceutical industry for years[17].

1.1 Quality by design and process analytical technology

Currently proposed strategies in good manufacturing practices of bio-pharmaceuticals are based on the Quality by Design (QbD) concept. QbD is a proactive approach in process development based on intensified process understanding[14,22]. QbD is described in several

guidelines by the International Council for Harmonisation of Technical Requirements for Pharmaceuticals for Human Use (ICH) published first in 2002[14]. The ICH guidelines relevant for QbD include *Pharmaceutical development (Q8)*[23], *Quality risk management (Q9)*[24], *Pharmaceutical quality systems (Q10)*[25] and *Development and manufacture of drug substances (Q11)*[26,27]. The guidelines are strongly supported by European Medicine Agency (EMA) and U.S Food and Drug Administration (FDA) with the higher goal of market harmonization and facilitation of regulatory decisions[28].

Complementary to QbD, the framework Process Analytical Technology (PAT) was introduced by the FDA in 2004 as guidance for industry[13]. PAT is a system for designing, analyzing, and controlling manufacturing processes. This shall be accomplished by real-time monitoring of critical quality attributes to ensure overall product quality[13,17]. The concept of PAT for process analysis and control has already been present in the field of chemical engineering for decades[29–31]. It can be regarded as real-time quality assurance in pharmaceutical manufacturing[17] and facilitate validation and process control for regulatory requirements[13]. Practical tools of PAT are for example multivariate tools for design, data acquisition and analysis, analyzers, process control tools and continuous improvement and knowledge management tools[13].

Both QbD and PAT were designed to support and relieve process development by process understanding while ensuring inherent safety and quality of pharmaceuticals[13]. Process understanding is presumed if *'(1) all critical sources of variability are identified and clarified, (2) variability is controlled by the process and (3) product quality attributes can be accurately and reliably predicted over the design space specified for the materials, process parameters, manufacturing, environmental and other conditions used'* according to PAT. Being able to make predictions is representative for a high degree of process understanding[13]. Moreover, the QbD concept is regarded as inherent quality risk management (QRM) since it is a systematic and integrated approach[27]. In application the QbD approach suggests the definition of the quality target product profile (QTPP), the critical quality attributes (CQA) which impact clinical efficacy or safety and the assessment of relevant process parameters in the overall process[14,17,32]. The relation between the critical process parameters (CPPs) and product quality attributes is evaluated in statistical Design of Experiments (DoE), multivariate data analysis and mathematical modelling techniques. The process operation space can therefore be defined and critically monitored[17]. In PAT and within the ICH Q8 guidelines it was stated that '*Quality cannot be tested into products; it should be built-in or should be by design*'[13,23] and discussed at numerous occasions ever since[28,33–36]: Contrary to the enforced QbD concept there is no golden standard of implementation yet and adoption of PAT in industry is not progressing as expected years ago. Only in 2013 the first QbD process was approved for the

monoclonal antibody Gazyva® of Roche[37,38]. The hesitant progress is often reasoned by rigid regulations in pharmaceutical industry and regulatory uncertainties during process development in comparison to other fields of industry[12]. Contrary, the conventional approach of batch processing and extensive product testing has been successful for a long time and is also referred to as Quality by Testing (QbT) approach[17]. Thus, mainly repetitive batch processes are produced, which variabilities are mostly prone to biologic material and not the batch processes[35,39]. Consequently, the industrial production of bio-pharmaceuticals is restricted to fixed process conditions, raw material characteristics and extensive end-product testing[17,35,39]. Also, bio-pharmaceutical manufacturers still justify the QbT approach by the complexity of bio-processes[35] and lack of appropriate real-time measurement tools[39]. The QbT situation is limiting the development of biopharmaceutical products and respective processes[40,41]. Especially in the growing interest in continuous manufacturing[42], merely off-line testing of raw materials and the end-product is currently feasible[41]. PAT is considered as challenging but crucial for future development strategies[12]. To close the gap to QbD, real-time measurements providing information about the process and the quality attributes of the product are required[35]. Novel sensor-technologies are proposed within this thesis as useful tools in PAT and according to QbD[12,17,35,43].

1.2 Soft sensing

In upstream bio-processes, on-line monitoring of pH, temperature and dissolved oxygen is state of the art[17]. The design of sensors is limited by the measuring principle which can be directly translated into the desired output variables. Soft sensing techniques offer advantages by translating unspecific measurements from sensors to bio-process variables[44]. These can be designed rather simple and have no need of high-end devices[17]. The term soft sensor originates from industrial process monitoring and is composed of the terms "software" for signal evaluation models, which are usually based on computer programs, and "sensor" for providing information similar to hardware sensors[45]. This is visualized in a process scheme on soft sensors in Figure 1.

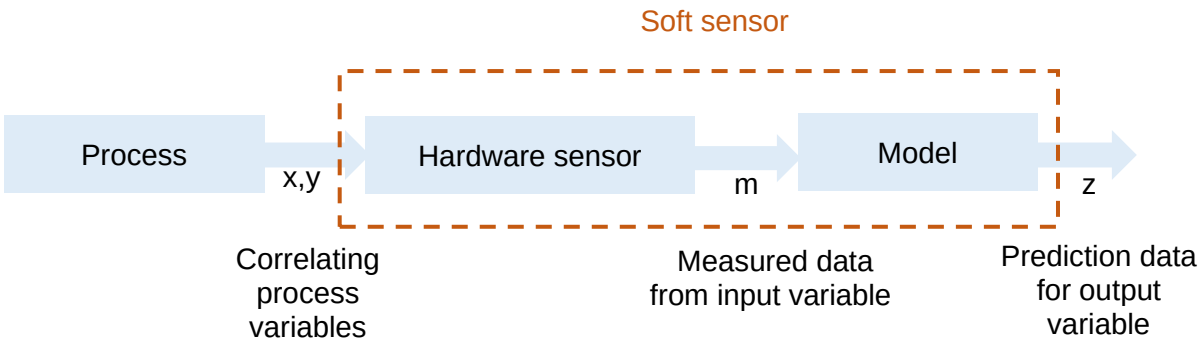

Figure 1: Soft sensor process scheme adapted from Luttmann et al.[44]

Soft sensors can be differentiated by the principle they are based on: Model-driven or data-driven. Model-driven soft sensors are usually based on First Principal Mode, which take chemical and physical relations into account and describe ideal processes whereas data-driven soft sensors are based on data from real processes. Therefore, data-driven soft sensors describe the process conditions more realistically but cannot be used to extrapolate outside the initial dataset used to build the data-driven soft sensor[45]. The term soft sensor may imply data evaluation as on-line measurements, but the idea of on-line measurement should rather be expanded. Thereby, the measurement of on-line data that is otherwise difficult to measure or only measured at low frequency[44] e.g. cell counting in mammalian fermentation should be included. As these variables are often related to the quality of the process and are CPPs, they are crucial for process control and management. For these reasons it is of great interest to provide additional information about these variables at a higher sampling rate and/or lower financial burden, which is precisely the task of soft sensors[45]. Only a few soft sensors have been recorded in the field of biotechnology[46] although more than 1.000 soft sensors have generally been published in the field of engineering[47]. One established example for QbD/PAT tool is an on-line sensor for NIR spectroscopy. It can determine the active pharmaceutical ingredient concentration in a blender output stream in real-time and improve the formulation of the Tablet[16,48].

Especially in cost-driven upstream processing, soft sensors offer numerous extensions to available sensors by translating measurements in aspired and non-directly measurable variables e.g. cell and product concentration.

1.3 Products and cell factories in upstream processing

By 2024, the global biologics market is expected to reach nearly 400 billion US dollars[49] with monoclonal antibodies accounting for top-selling drugs for the last decades[50,51].

Monoclonal antibodies

Monoclonal antibodies (mAbs) and other recombinant proteins are effective therapeutics and target various diseases[52]. Currently most mAbs treat cancer and immune-mediated disorders[53]. Further driving factors in the success of mAbs are the increased understanding of diseases on their molecular level, instead of simply combating symptoms and the high public acceptance[54]. The first mAb was approved by the FDA in 1986[50] and by 2020, approval of 70 mAb products was expected[55]. However, the market has grown even more rapidly leading to 131 approved mAbs only one year later (in 2021) for the European and U.S. American market, excluding biosimilars, Fc fusion proteins and emergency use authorizations[53]. Additionally, the global population growth and aging accompanied with emerging chronic diseases such as cancer, underline the necessity of bio-pharmaceuticals. Besides that, mAbs targeting neuro-

degenerative and inflammatory diseases like dementia, parkinson and arthritis play a promising role[56]. Production of mAbs and most recombinant proteins is performed in mammalian cell culture[56-59]. Especially mAbs require certain post-translational modifications (PTMs) which are possible in mammalian cells but lacking in other cell factories[57,60,61]. In particular glycosylation is crucial for therapeutic efficacy and safety and needs to be human-like[56,57]. The synthesis of mAbs is based on a suiTable expression vector which carries the transfected DNA[56,62]. Further steps are translation of antibody mRNAs, assembling, PTMs and secretion[57]. In research, product yields of up to 10 g/L have been reported[63] and may be even further increased.

Chinese hamster ovary cells

Chinese hamster ovary (CHO) cells are considered a workhorse in bio-pharmaceutical industry and are mainly used to produce mAbs[56,64,65]. CHO cells are derived from chinese hamster ovarian fibroblast cells and have been further developed to various cell lines with different features. CHO cells offer enormous adaptability by allowing suspension cultivation in chemically defined medium at high densities[66]. The absence of serum leads to cost reduction, less risk of viral or prion contamination and facilitated downstream processes due to fewer protein contaminants[67]. Since CHO cells are not human-derived cells, they are less prone to human virus infections and thereby increase biosafety[68]. Yet, genetic variability in CHO cells has been reported and requires attention to prevent drawbacks[69]. However, this leads to opportunities in cell line development for mutant lines lacking certain metabolic enzymes[70].

Human embryonic kidney cells

Another well-established mammalian cell line is the HEK293 cell line derived from human embryonic kidney cells. HEK293 was developed almost two decades after the CHO cell line and was the first human cell line transformed with adenovirus DNA fragments[71]. Subsequently, various sub cell lines of HEK293 have been established for adaption to suspension culture (HEK293 N3S[72]), serum free conditions (HEK293-S[73]) and improved transient gene expression (HEK293-T[74], HEK293-E[75]). HEK cells are one of the most used human cell lines for protein production as their PTMs lead to human-like proteins[76]. Production improvements has led to mAb titers of at least 1 g/L for transient transfections[77] while stable cell line development or rational vector design offer chances for further titer increase[78].

Insect cells

Insect cells with the baculovirus expression vector system gained importance in academic research for novel platforms in recombinant protein[79,80], virus[81] and virus-like particles[82] production. Also, the production of glycoproteins which are ‘mammalianized’ in their N-glycosylation is of great interest for therapeutic applications[79,83]. Advantages of insect cell

lines are serum free cultivation, higher tolerance to osmolality and by-product concentration as well as higher expression levels[79]. One widely used insect cell line is High Five™ (BTI-Tn-5B1-4), derived from ovarian cells of *Trichoplusia ni* (Tn) and developed by the Boyce Thompson Institute for Plant Research[84–86]. In High Five™ cells, higher titers of recombinant protein production were obtained compared to other insect cell lines such as Sf9[87,88]. One advantageous sub clone of High Five™ is the Tn*ms*42 cell line which is free of latent nodavirus infection contrary to previously mentioned Tn cell lines[85,86,89–91].

In upstream processing, determination of biomass or viable cell density is crucial and is therefore constant improved is focused[92].

1.4 Methods for in-situ cell counting

Reliable in-situ cell counting for biomass determination in fermentation processes has not been solved and is rarely found in industrial applications, although many prototypes and one-time applications have been developed[92]. For successful application, probes must provide calibration, linear dependency, and precision at low and high cell densities[93] as well as technical suitability for in-situ applications. The latter demands probes to be sterilizable, endure temperature and pressure, be corrosion resistant and biologically inactive and be consistent over multiple fermentation cycles[94]. Several methods and their challenges are:

Optical density probes

Optical density probes are often used in in-situ applications and are based on an organism specific wavelength. While cell types and morphologies influence the measurements, remarkable errors result from the size and amount of air bubbles in a bioreactor[95]. This can be overcome by using a degassed measurement chamber, but the additional construction may affect cleaning in place (CIP) results[93]. Different probes have been investigated for backscattering and transmission measurements and they are either in favor of low or high cell densities. Regarding practical implementation, the possibility of probe fouling must be considered and should therefore be critically monitored[92].

Dielectric spectroscopy

Dielectric spectroscopy is used for measuring the change in capacitance or the relative permittivity of the fermentation broth and is a well described principle[96–98]. Thereby, a pre-amplifier near the probe is required to compensate for the weak signal. The capacitance is measured at different frequencies and creates a dielectric spectrum of the cell suspension which is influenced by the cell concentration and media components[97]. Although several cell lines, including mammalian[99,100], have been investigated in previous research, the main industrial application is currently in breweries. As limitation, most publications are either directly or indirectly based on Aber Instruments Ltd[92].

Infrared spectroscopy

Infrared spectroscopy can be applied in near infrared (NIR), mid-infrared (MIR) and the whole infrared range and can obtain more process information besides biomass concentration. The measurement is typically performed at-line or online by medium circulation systems and data processing and advanced analysis algorithms are required[92]. In in-situ applications, fiber optic probes are applied where the probe path length is crucial for accuracy[101]. Similar to other methods mentioned previously, agitation and aeration are reported to affect the measurements[102].

Fluorescence

Another method for determining biomass is based on fluorescence, specifically on excitation by UV light at a certain wavelength and measuring emission of culture components at another wavelength. The first application was already published in 1970 and numerous more have followed[92,103]. However, challenges remain as the method is restricted to viable cells, constant NAD(P)H amount per cell and fixed culture conditions[104]. As major drawback, certain medium components may interfere with fluorescent detection and require further 2D fluorescence spectroscopy[93] which still leads to 10% estimated errors[105,106].

Calculation methods

In a different perspective, calculation methods based on correlation or software sensors are investigated. In terms of correlation, numerous variables from available probes and data have been linked to cell counts by stoichiometric coefficients and modeling: demand on pH control, conductivity[107–109], broth viscosity[110], heat balances[111–114] and most often off-gas analysis[115-119]. Mathematical models resulting in software sensors are usually based on growth kinetics or statistical analysis. However, kinetics-based biomass estimation is often not applicable to bioprocesses as constant coefficients cannot be assumed[92].

The oxygen uptake rate (OUR) in mammalian cell culture is an indicator for metabolic activity and has been a starting point for further in-situ determinations of cell growth in the last years of upstream development[120–122].

1.5 Oxygen uptake rate

The OUR and CO_2 production rate (CPR) were already of great interest for decades and investigated by off-gas measurements via mass-spectrometers and quantified by their flow rates[123–125]. However, off-gas measurements have not been widely implemented due to the high acquisition costs and the complexity of the devices, which require equally skilled personnel[126]. In 2011 a simplified off-gas analysis for OUR determination in animal cell culture was published with single gas sensors for measuring O_2 and CO_2 and thereby replacing mass spectrometers[126]. The experiments were conducted with CHO mAb producing cells and pH

regulation with acid and base to exclude influence of additional CO_2. In the advanced application, the OUR was implemented in a cascade controller in an industrial process control system Simatic PCS 7 (Siemens AG) to establish desired growth rates continuously[127]. Also, Desphande and Heinzle determined the oxygen consumption rate of CHO cells with fluorescent O_2 sensors in 96-well plates[128]. Thereby, CO_2 incubation was abandoned as well and further buffering reagents were added. A drawback of this sensor is the at-line measurement where a sample of cell suspension is transferred to the microtiter plate.

In 2019, soft sensing of viable cells via dynamic $k_L a$ computation was introduced as new approach[129]. The $k_L a$ is the volumetric mass transfer coefficient and describes the transport of oxygen from gas bubbles to each cell in a bioreactor. In combination with the oxygen concentration gradient ($c_L{}^* - c_{O_2}$), it can be used to define the gas-liquid transfer rate and the oxygen transfer rate (OTR) (Equation 1)[130].

$$OTR = k_L a * (c_L{}^* - c_{O_2}) \quad (1)$$

However, one major challenge is precise calculation of OTR during a bioprocess, as this parameter is varying and complex. Especially pressure and temperature are affecting the OTR[130,131], but also the stirrer speed, gas flow and media properties in combination with the chosen operation mode. In terms of media properties, several more factors come into play: The concentration of electrolytes may enhance $k_L a$ by suppressing bubble coalescence, while high concentrations of common additives for shear protection as Pluronic F68 may reduce the bubble size[132]. In addition, antifoam agents like silicone oils may increase oxygen transfer[133]. During the bioprocess, an increase of biomass particle size and by-product formation may also reduce $k_L a$ values due to enhanced bubble coalescence[134].

A dynamic model for $k_L a$ was developed by investigating different variables (process air and CO_2 inlet gas flow-rates, temperature, volume, pressure) in a 15 L bioreactor and their influence on $k_L a$ and $c_L{}^*$. The model was applied to 13 fed-batch fermentations of mAb producing CHO cells to elucidate if the model can predict biomass prediction and the metabolic state based on OUR. It resulted in a two-segmented model due to variations of specific consumption of oxygen by metabolic transition: aspartate to glutamate ratio indicates this metabolic shift[129].

The sophisticated model raises the question if simplification through the dynamic OUR is feasible. The determination of dynamic OUR is proposed as short interruption of gas flow which leads to a directly measurable decrease of dissolved oxygen while neglecting $k_L a$[135].

1.6 Scripting in DASware®

In the DASware® Control Software of DASGIP® Parallel Bioreactor systems, fermentation processes can be designed in several ways: The process parameters are set internally when a standard process is chosen, but all parameters can be manually controlled as well. If one parameter shall be regulated in relation to another, a profile script can be written. Thereby, a function y(x) is determined where x is the profile source (e.g. inoculation time) and y the set-point to be controlled (e.g. temperature). If several parameters are required as source or are to be regulated, a reactor script can be programmed. Thus, more complex controlling is feasible e.g. for feed profiles based on base consumption. The programming language is Visual Basic.NET and is intellectual property of Microsoft[136] whereas the variables for process parameters and introducing literature are provided by Eppendorf. In Visual Basic.NET, the parameters are assigned to the global parameter variable `P` for object-oriented programming (`with P`). A few core concept building blocks usually available in all programming languages are presented here for the automation of the DASware®:

`If…Then…Else` Statement

A basic programming function is the `If…Then…Else` statement which conditionally executes a group of statements that are depended on a value of an expression. When `If` is encountered, a condition is tested: If the condition is `True`, the statements following `Then` are executed. If the condition is `False`, each following `Else` statement is evaluated in order. After executing the statements following `Then` or `Else`, execution ends with `End If`. The `Else` statement is optional and can be skipped, however it may ensure ongoing execution of the function for when the `If`-clause is not fulfilled (Figure 2). `If…Then…Else` statements can also be nested within each other. Therefore, more than one condition can be tested by an `If-clause` and more precise execution of statements is feasible[137].

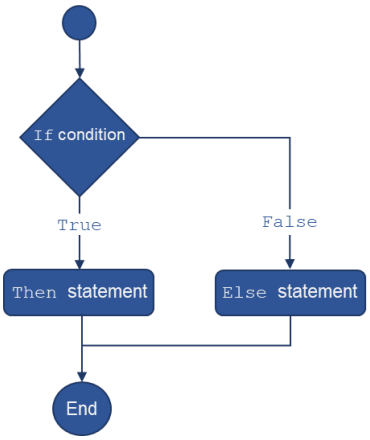

Figure 2: Execution of `If...Then...Else` Statement: If the test condition is `True`, statements following `Then` are executed. If the test condition is `False`, statements following `Else` are executed; figure adapted from Kühnel A.[137]

`Select Case` Statement

With the `Select Case` statement, different `Cases` can be executed depending on given expressions. By that, a script or process is clearly arranged in `Cases`. If an expression matches more than one `Case`, only the statements following the first match are executed. If no specified `Case` is matched, a `default Case` ensures ongoing of script execution. Each `Select Case` construction must have a matching `End Select` statement[137] (Figure 3). Additionally, `Select Case` constructions can be nested or advanced with `If…Then…Else` statements. Thereby, an `If`-condition is tested for `True` or `False` and for `True`, the matching case is executed. This allows more precise execution.

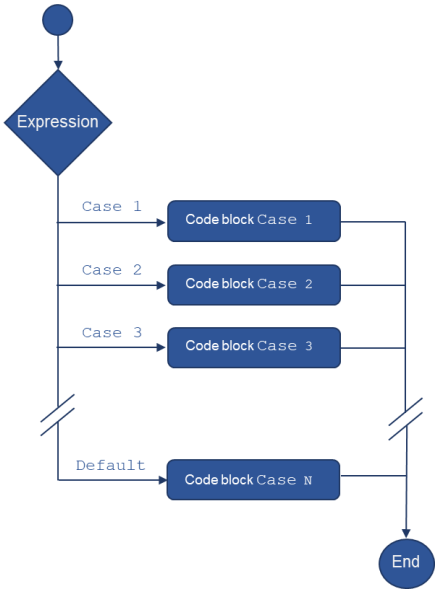

Figure 3: `Case Select` statement: The first `Case` to match an expression is executed; figure adapted from Kühnel A.[137]

Unix Epoch Time

For referencing time within the DASware®, one option is to use an absolute time available within Visual Basic, the so-called Unix Epoch time. The Unix Epoch time started on January 1st, 1970, at UTC and runs in seconds. In the DASware® Control Software 26 internal values A-Z are available as space holders for e.g. off-line values. These can be used to import the Unix Epoch Time and make it available for process control. Thereby, numeric timestamps can be set and these timestamps can be manually controlled to any second of the Unix Epoch time. Hence, high flexibility which is required for trouble shooting is given.

1.7 Objective of this thesis

A non-invasive soft sensor for simplified on-line cell counting based on dynamic oxygen uptake rate can close the gap to QbD and PAT for upstream viable cell concentration measurements. The main objective of this thesis is the measurement of dynamic oxygen uptake rates in CHO fed-batch processes by automated and periodic interruptions of gas supply in DASGIP® bioreactors to develop a soft sensor for viable cell count determination. This thesis works under the hypothesis that the oxygen uptake rate is directly proportional to the viable cell concentration in the bioreactor. Additionally, the thesis has to prove that changing dissolved oxygen concentrations do not influence the process as a whole, as the soft sensor requires the periodic interruption of the gas supply. This also requires that the gas supply is reactivated dynamically to resume at a certain minimum oxygen concentration to avoid oxygen starvation of the cells. Lastly, the thesis has to correlate the dynamic oxygen uptake rate and cell number using off-line measurements, and answer the question if the methodology is transferable to other cell systems is examined. The development of such a soft sensor is crucially important for the development of the QbD/PAT sensor, as it is the first presented sensor that does not need any specialized additional equipment (like off-gas analytics) or the extensive characterization of the $k_L a$ of the system under all relevant volumes, gassing, mixing and viscosity conditions that occur during a process. This new soft-sensor methodology relies solely on the direct measure of oxygen consumed by the cells in the bioreactor, and does not need any physical modification of the reactor and only needs software modification for the control software. It can also be implemented in any form of bioreactor, for any process and any scale as long as the process already uses a probe for dissolved oxygen, without needing additional equipment or sensors. To develop this new soft sensor for simplified on-line cell count measurement 3 main objectives need to be achieved:

- The full automation of the gas supply to program a periodic interruption that re-activates the gas supply when reaching a minimum dissolved oxygen concentration
- The proof that gas supply changes necessary for the soft sensor do not change the growth characteristics of the culture
- The correlation of oxygen consumption during interrupted gas supply phases with viable cell concentration measured off-line to complete the on-line soft sensor

2. Material and methods

The soft sensor is developed in upstream processes for which cell culture fermentations are required. Further sampling and analytic strategies for soft sensor development, process monitoring, and investigation of the influences of the soft sensor methodology are stated. All solutions were prepared with 0.22 µm filtrated RO-H_2O (E-POD® with Millipak® Express 40 filter, 0.22 µm) and sterile vacuum filtered in 500 mL or 1000 mL single use units (Nalgene™ Rapid-Flow™).

2.1 Process setup

The experiments in this thesis necessitate comparable processes with automated gas flow interruptions by script application for soft sensor development and control. For that, a setup was established.

Bioreactor

The fermentation processes were performed in DASGIP® Parallel Bioreactor Systems (Eppendorf) with 1.5 L vessels. The headplate setup was sufficient for the respective probes and in-/outlets and tubes were attached via Luer-Lock system for sterile connections. A detailed overview is given is Table 1.

Table 1: Bioreactor complementation

Component	Specification	Supplier
Stirrer	maxon motor	Eppendorf
pH probe	EasyFerm Plus K8	Hamilton
DO probe	VisiFerm DO ECS 325	Hamilton
Temperature probe	pT 100	Eppendorf
L-sparger		Eppendorf
Vent air filter	0.20 µm, PTFE membrane	Millex®-FG
Off-gas filter	Acropak 300, PTFE membrane	Pall
Dip tube combined with reflux filter for sampling	0.20 µm, PTFE membrane	Sartorius
Reflux condenser		Eppendorf
Dip tube for harvest		Eppendorf
Ports for addition of medium, inoculum, base, acid/antifoam		Eppendorf

A layout of the head-plate setup is given in Figure 4.

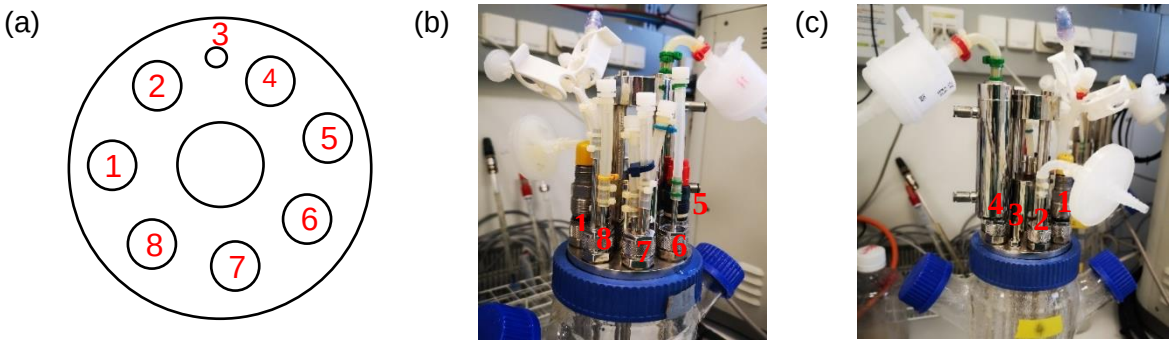

Figure 3: DASGIP® Headplate (a) scheme (b) front (c) back): DO probe (1), vent air filter on sparger (2), dip tube for temperature probe (3), reflux condenser (4), pH probe (5), dip tube for harvest (6), combined port for addition of medium, inoculum, base (7), addition of base/acid/antifoam (8)

Calibration protocols for pH (pH 4 and pH 7) and DO probes (0% with N_2 and 100% with air) were added to each unit in the DASware® Control Software (Eppendorf) and performed prior sterilization with calibration buffer solutions (Certipur®) and RO-H_2O for pH and DO respectively. After sterilization at 121°C for 20 minutes the RO-H_2O was discarded through the harvest tube and 350 mL media were added. For sterility testing the media was held at the respective fermentation temperatures for at least 24 h. The total working volume of 600 mL was adjusted after inoculation.

Script application

A script was developed for periodic and automated gas flow interruptions for dynamic OUR measurements as variable of the soft sensor. Both periodic repetition and dynamic regulation of the gas flow interruption at a certain lower dissolved oxygen concentration were included to prevent oxygen starvation of the cells at development stage.

Through incremental steps, the final script can stop the gas flow for a certain time or until a certain threshold in %DO is reached. The aeration was interrupted every 3 h for 10 min or until 30 %DO were reached. The script in Source code 4 is described in 3.1 Script development.

2.2 Fermentation

Fermentations of HEK293, CHO and Tn*ms*42 cells were performed based on established parameters except the gas flow rate and %DO set point. These were varied by the script for automated gas flow interruptions for soft sensor development. The bioreactor vessels were divided between fermentations running with the script implemented for soft sensor development and fermentations without implementation. The latter serves as control. For each of the cell lines tested, two runs with two to four individual vessels each were performed with half of the vessels running with and half of them running without the script implemented.

Mammalian cell culture – HEK293

Frozen cell bank vials (cell concentration was 1×10^7 cells/mL) were thawed and suspended in 9 mL fridge cold FreeStyle™ F17 medium (Gibco) supplemented with 8 mM L-Glutamine (200 mM stock solution, Sigma-Aldrich) and 0.1% Pluronic® F-68 (10% solution, Gibco) in a falcon tube. After centrifugation (300 g, 5 min; Eppendorf Centrifuge 5910R), the supernatant was discarded and the cell pellet gently resuspended in 10 mL pre-warmed medium. The cell suspension was diluted to 20 mL medium and cultivated in 125 mL shaking flasks (0.2 µm vent cap, nonpyrogenic polycarbonate, Corning). Expansion for fermentation was in 500 mL vented shaking flasks (0.2 µm vent cap, nonpyrogenic polycarbonate, Corning). The cells were cultivated in a CO_2 incubator (BBD 6220, Thermo Scientific) at 37°C, 8% CO_2, 130 rpm and 80% humidity. Cell densities from 0.4×10^6 cells/mL to 2.5×10^6 cells/mL were maintained by passaging three times a week. Inoculation concentration for the bioreactor was 0.5×10^6 cells/mL. A medium exchange before inoculation was achieved through centrifugation (300 g, 5 min; Eppendorf Centrifuge 5910R) and carefully resuspending in fresh medium prior to inoculation. The pH control was based on CO_2 and base addition using 7.5% sodium bicarbonate (Sigma-Aldrich). An appropriate 10% glucose feed (Carl Roth) were added to maintain a glucose concentration of at least 2 g/L. Additional fermentation parameters are listed in Table 2.

Table 2: Operating parameters for mammalian cell culture

Parameter	Setpoint
Stirrer speed	60 rpm
pH	7.2
Temperature	37°C
DO	60%
Gas flow rate	3 sL/h

Mammalian cell culture – CHO

Frozen cell bank vials of CHO K1 producing IgG1 Adalimumab were thawed as previously described in HEK293 cells. Additionally, 0.5 mL of 50 mg/mL stock solution Geneticin G-418 Sulphate (Gibco, filtered by Millex®-GV, 0.22 µm, sterile) and 25 µL Anti-Clumping agent (Gibco, 1:1000 dilution) were added in the first passage. The cells were cultivated in ActiPro™ medium (HyClone™) supplemented to 8 mM L-Glutamine (200 mM stock solution, Sigma-Aldrich) in 125 mL vented shaking flasks (0.2 µm vent cap, nonpyrogenic polycarbonate, Corning). Culture conditions were as previously described (*Mammalian cell culture - HEK293*). Cell densities from 0.3×10^6 cells/mL to 2.5×10^6 cells/mL were maintained by passaging three times a week. The cells were expanded in 500 mL vented shaking flasks (0.2 µm vent cap,

nonpyrogenic polycarbonate, Corning) to reach an inoculation density of 0.5×10^6 cells/mL. No medium exchange was performed, which resulted in 15-23% conditioned media at the time of inoculation. The pH control, feeding strategy and additional fermentation parameters were as previously described in HEK293 cells.

Insect cell culture

Frozen cell bank vials of Tn*ms*42 cells were thawed as previously described in HEK293 cells and first cultivated adherently in cell culture flasks with FSM4 Insect™ media (with L-Glutamine, Cytiva, HyClone™). Passaging was performed at app. 90% confluency every two to three days for two weeks before transferring to suspension culture and adaption for two further weeks. Cell densities from 0.35×10^6 cells/mL to 2.5×10^6 cells/mL were maintained by passaging three times a week in 100 mL glass shaking flasks (Schott Duran). Culture conditions in the incubator and shaker (GFL 3033) were 27°C and 110 rpm. The cells were expanded in 500 mL glass shaking flasks (Schott Duran). The inoculation density was 0.6×10^6 cells/mL. Media exchange was performed prior to inoculation (300 g, 5 min; Eppendorf Centrifuge 5910R). The pH control was based on acid (25% phosphoric acid, Sigma Aldrich) and base (7.5% sodium bicarbonate, Sigma-Aldrich) addition. An appropriate 10% glucose feed (Carl Roth) were added to maintain a glucose concentration of at least 2 g/L. Additional fermentation parameters are listed in Table 3.

Table 3: Operating parameters for insect cell fermentation

Parameter	Setpoint
Stirrer speed	200 rpm
pH	6.4
Temperature	27°C
DO	60%
Gas flow rate	0.3 sL/h

The transformation of the vessel script from mammalian to insect cell culture required adjustment of the standard gas flow rate from 3 sL/h to 0.3 sL/h.

2.3 Sampling and Analytics

Sampling timepoints for off-line analytics were made during gas flow stops. Up to three samples were taken at different timepoints per day. Sampling volume was 1 mL for cell density and viability analyses and 2×2 mL for product titer analyses, drawn aseptically with 5 mL Omnifix® syringes. For product titer analysis, 2×1.5 mL supernatant was frozen at -22 °C after centrifugation (1000 G, 3 min; Eppendorf Centrifuge, 5424) and filtration (0.22 µm Millipore Millex®-GV, Hydrophilic PVDF). In HEK293 and CHO fermentations, glucose concentration in the supernatant was measured by Wellion® CALLA light.

Cell counting and viability determination

Cell densities and viability were determined with a Vi-CELL™ XR cell viability analyzer (Beckmann Coulter) and a sample volume of 300-1000 µL. Cell concentrations above 1×10^7 cells/mL were diluted with PBS to meet the quantification range. CHO and Tn*ms*42 cells were measured with the in-house developed settings for CHO and Sf9 cells, respectively.

Titer determination

Chromatography A on HPLC (UltiMate™ 3000, Thermo Scientific™) was used with the according Chromeleon™ Software (Thermo Scientific™) for mAb titer determination. Details of the components and parameters are given in Table 4.

Table 4: Parameter and components of chromatography A method

Component or parameter	Specification					
Column	POROS™, Protein A 20 µm, 2.1 x 30 mm, 2-1001-00, ThermoScientific™					
Column storage	20% ethanol, 4°C					
Column temperature set-point	21°C					
Detection	UV/VIS: 280 nm, 214 nm					
Sample volume	50 µL					
Pressure	70 bar					
Binding buffer A	50 mM $NaPO_4$, 150 mM NaCl, pH 7					
Elution buffer B	100 mM Glycine, pH 2.5					
Run time	2.5 min					
Elution gradient	Time [min]	0.000	0.400	0.410	1.210	1.220	2.500
	%B	0.0	0.0	100.0	100.0	0.0	0.0

Analysis of chromatography peaks was performed using the Cobra wizard within the Chromeleon™ Software using the 280 nm signal. A calibration curve with standard triplicates of 25 µg/mL, 50 µg/mL, 100 µg/mL, 250 µg/mL, 1.000 µg/mL, 1.500 µg/mL and 1.670 µg/mL was provided by Komuczki D. and used for titer determination.

3. Results and discussion

The goal of this work was to develop a data-driven, on-line soft sensor for automated cell number determination that does not need any additional equipment for implementation. One way of determining the cell number is based on the oxygen consumption in the bioreactor and relating that value through a calibration to viable cells in the bioreactor. This cannot be done during normal operation of the bioprocess, as the oxygen content is held constant through regulation of inlet gas flow, inlet oxygen concentration and/or stirrer speed. A traditional method to determine this oxygen consumption is by a mass balance through gas inlet flow and composition and an off-gas analysis determining the composition of the off-gas. By using the differential between the two, the oxygen consumption of the culture can be determined, but this requires additional expensive equipment. Another traditional approach is the full characterization of $k_L a$ under all process conditions of gas flow, inlet oxygen concentration, stirrer speed, viscosity, filling volume etc. and calculation of the oxygen consumption based on the $k_L a$ model, using the current parameters and the resulting dissolved oxygen concentration. This requires a very extensive characterization of the bioprocess and is not transferable to other reactor shapes, production scales, different media or cell lines. To avoid additional equipment and extensive characterization, the soft sensor in this work uses an automated gas flow interruption and record the drop in dissolved oxygen to calculate the dynamic OUR. Since the soft sensor and its underlying model are data-driven, fermentation processes for model establishment were performed. The soft sensor model based on dynamic OUR values and the calibration were then done using off-line viable cell counts. Generating a gas flow interruption needs to be automated to make use of the concept as an on-line soft sensor, and therefore the DASware® software controlling the bioreactors used in this work (DASGIP®) was modified to implement an automated gas flow interruption. The DASware® software offers the possibility to include custom-made scripts that have access to all process variables during runtime and is based on Visual Basic.Net. This scripting capability was used in this work to develop and implement the soft sensor.

3.1 Script development

The script development was done in incremental steps, implementing the necessary features one-by-one into the script and testing the script performance after each iteration. The necessary features to be implemented in the script were gas flow interruptions for certain timespans, automated repetition of these cycles, and dynamic reactivation of gas flow at certain %DO process values to limit cell oxygen starvation.

Initial basic commands for gas flow regulation in Visual Basic.NET were tested on DASware® and DASGIP®. Then, several scripts were developed and investigated for automatic execution of gas flow interruption. The functionality of the scripts was examined by lowering the %DO

artificially with manual N_2 flow. Control messages within the scripts were added to observe execution of source code lines.

First, the variable inoculation time in hours (`InoculationTime_H`) was used in combination with a `Select Case` statement in Source code 1. In this approach, the variable `InoculationTime_H` specified when the gas supply was turned off (`InoculationTime_H > 3`). Switching between the flow states (`FSP`) was controlled in two `Cases`. In addition, the gas supply should only be switched off when the %DO (`DOPV`) had increased to 60% again, meaning that the culture returned back to its original setpoint. Switching on should be executed after 15 min or when the %DO decreased to 30% (`InoculationTime_H > 3.25 Or .DOPV < 30`).

Source Code 1: Script based on inoculation time and `Select Case` statement

```
With P
      If .InoculationTime_H > 3 And .DOPV > 60 then
        .Phase = 1
      elseif .InoculationTime_H > 3.25 Or .DOPV < 30 then
       .Phase = 2
      end if
      Select Case .Phase
      Case 1: .FSP=0
      Case 2: .FSP=3
      End Select
end with
```

The script successfully executed the task, however, since the variable `InoculationTime_H` is absolute in hours, the automated and dynamic repetition of gas flow interruption was not feasible.

Therefore, the `Do Loop` function was introduced as described in Source code 2. The new variable `LoopStart` was introduced and set to 0. In the outer loop, an `If`-clause included resolved nested executions when 60% DO were reached. Thereby, the variable `LoopStart` was set to the inoculation time as timestamp. In the following inner `Loop` function, the flow rate should be turned off continuously until the %DO drops below 30% or the time interval between the `LoopStart` timestamp and the process value of the inoculation time was exceeded. Further, `ElseIf` and `Else` cases were added to regulate the flow rate if none of the above regulation were initiated.

In this approach, the variable `InoculationTime_H` was not used in absolute values to enable continuous repetition. Thereby, the inbuild variable `Sampletime` which translates in ‘run the script only every x seconds’ was tested for applying the dynamic loops every 2700 s (3 h).

Source code 2: Script based on `Do Loop` functions

```
With P
      .Sampletime = 2700
      Dim LoopStart as double
      LoopStart = 0
      Do
            If .DOPV > 55 then
                  if LoopStart = 0 then
                  LoopStart = .InoculationTime_H
                  Do
                        .LogMessage("Phase 2")
                        .FSP = 0 while .DOPV < 30 and .InoculationTime_H
                        - Loopstart > 0.25
                  Loop
                        .LogMessage("Phase 3")
                  end if
            ElseIf .DOPV < 45 then
                  .FSP = 3
            Else .FSP = 3
            End If
      Loop
end with
```

As the `Do Loop` function executes statements such as the `LogMessage` every second, the DASware® ultimately froze. The variable `Sampletime` started the script after 3 h but investigations showed that scripts in DASware® are run every 10 s regardless and thereby all applicable statements are evaluated. It is likely that the `Loop` function accelerated the execution of the script which froze the DASware®.

A new approach in Source code 3 introduced a `Timer` to enable time-dependent execution. This `Timer` function requires several new variables which were introduced such as `Timer`, `timer.Interval`, `timer.Elapsed`, `timer.Autoreset`, `Timer.Enabled` and `Timer.Start`. Complementary to previous approaches, `If`, `ElseIf` and `Else` clauses for selecting cases in gas flow regulation were added as this had already been successfully integrated.

Source code 3: Script based on timer

```
Dim timer As Timer = New Timer ()
timer.Interval = 600000
AddHandler timer.Elapsed, New ElapsedEventHandler (AddressOf
TimerElapsed)
timer.AutoReset = True
timer.Enabled = True
timer.Start ()
with P
      if .DOPV > 60 then
            .Phase = 1
      elseif .DOPV < 30
            .Phase = 2
      else .FSP = 3
      end if
Select Case .Phase
Case 1:  .FSP = 0
Case 2:  .FSP = 3
End Select
end with
```

Intensive testing of the given variables showed that they could not be identified. In conclusion, the `Timer` commands did not apply to the available Visual Basic version in the DASware® meaning that not the full functionality of Visual Basic.Net is available in the Software, even if that is not stated in any documentation available by the manufacturer.

Alternatively, the absolute Unix Epoch Time was introduced for time-dependent regulation. Two internal values A and B, otherwise set to 0, serve as space holders for timestamps in Unix Time. Source code 4 was successfully developed and manages interruptions of the gas flow for a certain time or until a certain threshold in %DO is reached.

Source code 4: basic commands (black), Unix Timestamp if-clauses (purple), `if`-clause (blue), nested-`if`-clause (green), Unix timestamp actualization (pink), `Case Select` function (red)

```
with P                                                                    (1)
.FSP = 3                                                                  (2)
      if .IntA = 0 then                                                   (3)
          .IntA = DateDiff("s", "1/1/1970 00:00:00", Now())               (4)
      end if                                                              (5)
      if .IntB = 0 then                                                   (6)
          .IntB = DateDiff("s","1/1/1970 00:00:00",                       (7)
        Now())+10800
      end if                                                              (8)
      if DateDiff("s","1/1/1970 00:00:00",Now())-.IntA >                  (9)
      10200 then
            .Phase = 1                                                    (10)
            if DateDiff("s","1/1/1970 00:00:00", Now()-.IntB >            (11)
            or .DOPV < 30 then
                .LogMessage("Phase2")                                     (12)
                .IntA  = DateDiff("s","1/1/1970 00:00:00",Now())          (13)
                .IntB  = .IntA + 10800                                    (14)
                .Phase = 2                                                (15)
            end if                                                        (16)
      else .Phase = 2                                                     (17)
      end if                                                              (18)
      select Case .Phase                                                  (19)
      Case 1: .FSP = 0                                                    (20)
      Case 2: .FSP = 3                                                    (21)
      end select                                                          (22)
end with                                                                  (23)
```

Source code 4 shows that the script is written based on the global parameter variable `P` for accessibility of parameters (1, 23). The gas flow rate must be set to a certain volume in the beginning (2). In default setting, the Internal Values A (`IntA`) and B (`IntB`) are 0. A respective `If`-clause can be used once to import Unix Time with `DateDiff` function (3-8). `IntA` is set as current Unix Time (3-5) whereas `IntB` is set as current Unix time plus 10 800 s or 3 h (6-8). As soon as the difference between the continuing Unix time and the `IntA` exceeded 10 200 s, after 2 h and 50 min respectively (9), `Phase 1` is activated (10). This leads to `Case 1` and gas flow shut-off (19-20). As soon as the continuing Unix time is higher than the `IntB` or the %DO is below 30 (11), further functions are executed: The `LogMessage` "Phase 2" confirms the procedure (12). `IntA` is updated to the current Unix Time (13) and `IntB` is updated to `IntA` plus 3 h. Then `Phase 2` can be selected (15) and `Case 2` with gas flow rate turned on is executed (19+21). As the continuing Unix time is again 2 h and 50 min past the updated `IntA` the gas flow will be stopped for 10 min or until 30 %DO are reached (9-22).

Final optimizations were implemented after the first fermentation and the aeration was interrupted every 3 h for 10 min or until 30 %DO were reached.

3.2 HEK293 fermentations

Suspension adapted HEK293 cells were the first cell system to be investigated in fermentation processes and dynamic OUR measurements. Therefore, evaluation of the established fermentation parameters is crucial to acquire robust and successful processes for dynamic OUR measurements and further soft sensor development. Thus, HEK293 fermentations were used as preliminary experiments to assess the possibility of dynamic OUR measurements, improve time intervals and data collection timeframes, and investigate script implementation for soft sensor development.

Two cell bank vials of HEK293 cells were thawed and each used for a fermentation process. The first fermentation of HEK293 cells was run with four parallel vessels prior to the script development as a basic fermentation process and data collection for later comparability (Figure). However, the cells were not growing properly in three of the vessels, which is also reflected in the viability data. Therefore, the fermentations in three vessels were terminated after 110 h. Only one vessel reached a viable cell concentration (VCC) of 3.6×10^6 cells/mL after 7.7 days despite a constantly decreasing cell viability to below 80%. Since only this vessel had an initial concentration of 0.5×10^6 cells/m and other vessels were inoculated with lower cell concentration, a higher inoculation density was aimed in the following fermentations.

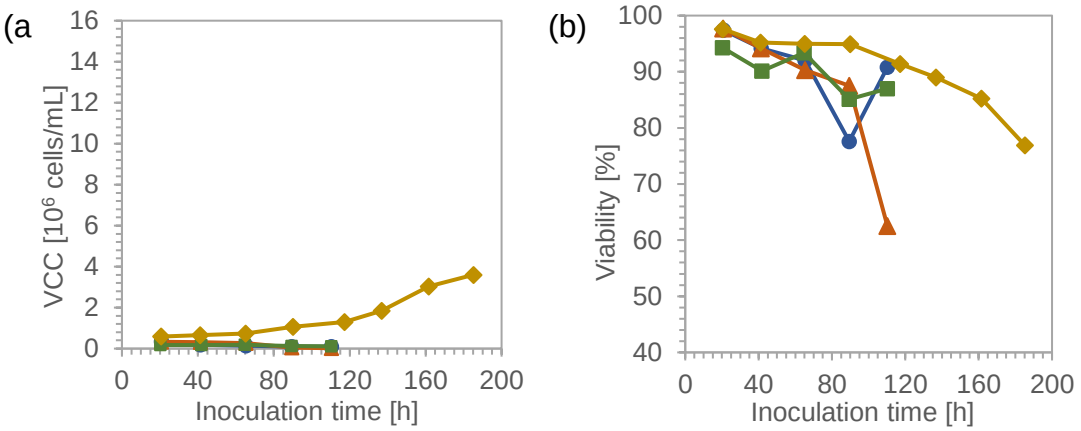

Figure 4: HEK293 fermentation without applying the script, displaying four vessels in (a) VCC [10^6 cells/mL] (b) viability [%] over inoculation time [h]

Furthermore, the principle of measuring the dynamic OUR by manual gas flow interruption was investigated in the vessel with highest VCC (Figure 5). Thereby, several observations could be made: The process values of %DO decline already after several seconds of gas flow interruption despite low cell densities between 0.5 – 1×10^6 cells/mL. Already at this preliminary test, a correlation between the %DO drop per time and cell density was visible (Figure 5 (a)). From the default settings the data collection interval is 15 min which is not sufficient since the linear %DO drop can be measured within a few minutes. For the initial results this resulted in a bias (Figure 5 (b)), as only two process data points are available during gas flow interruption,

leading to deceptive time frames of %DO drop and the gas flow rate. Furthermore, gas flow interruptions cause over regulations to reach the set point once the gas flow is switched back on but the following underregulation does not exceed a critical lower limit of %DO. The integral part of the PID regulator was reduced from 300 s to 100 s in the beginning to enable more precise regulation. The complete stabilization of %DO lasts app. 3h.

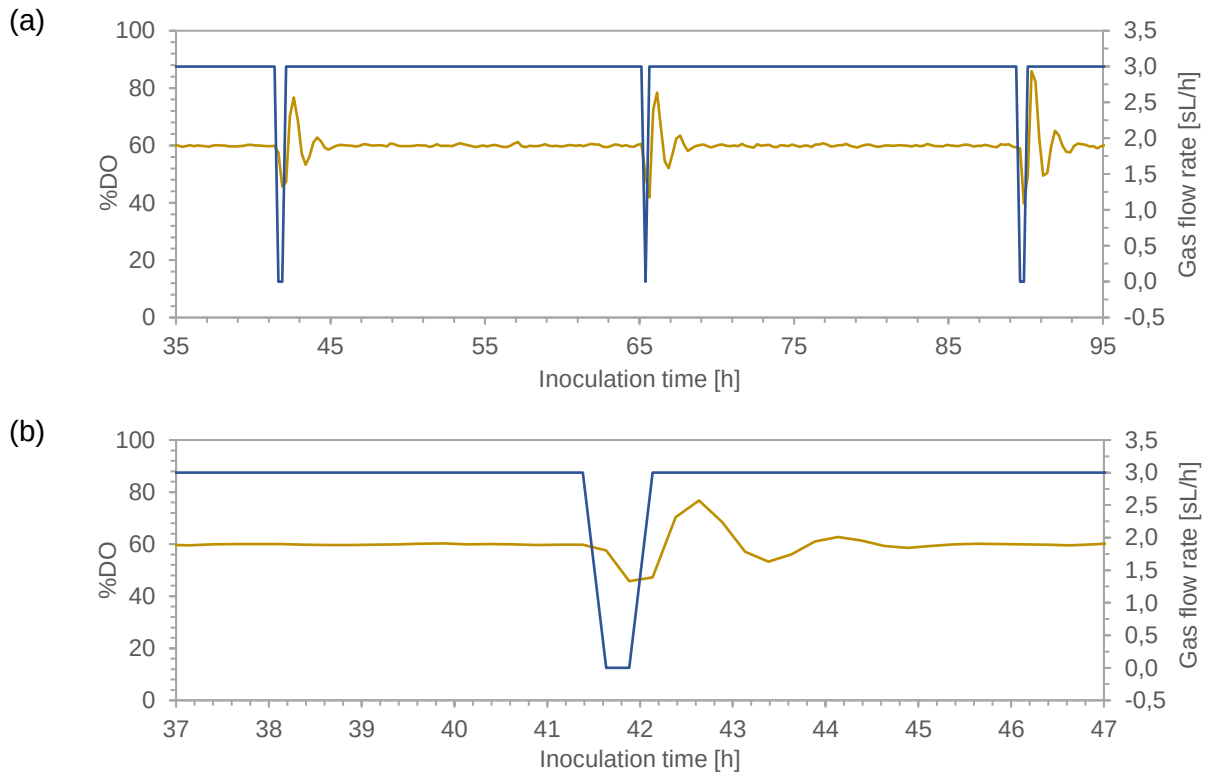

Figure 5: Manual gas flow interruption in one vessel of first HEK293 fermentation with %DO process values (beige) and gas flow rate (blue) displaying (a) several gas flow interruptions between 35-95 h inoculation time and (b) closeup of first gas flow interruption

In the second fermentation of HEK293, the theoretical inoculation density of 0.5×10^6 cells/mL was aimed at and an additional safety buffer of 20% inoculum and thorough flushing during the media exchange was done to make sure all of the inoculum was transferred to the reactor. Thereby, inoculation densities of $0.45 – 0.6\times10^6$ cells/mL were reached in all vessels. The developed script was applied in half of the vessels prior to the first cell density measurement.

In all vessels, HEK293 cells did not exceed a cell concentration of 1×10^6 cells/mL after 90 h. However, the viability in all vessels did not decrease below 90%. In further detail, slightly lower cell densities were determined in the vessels where the script was applied which may be due to lower inoculation densities of 0.45×10^6 cells/mL (Figure 6).

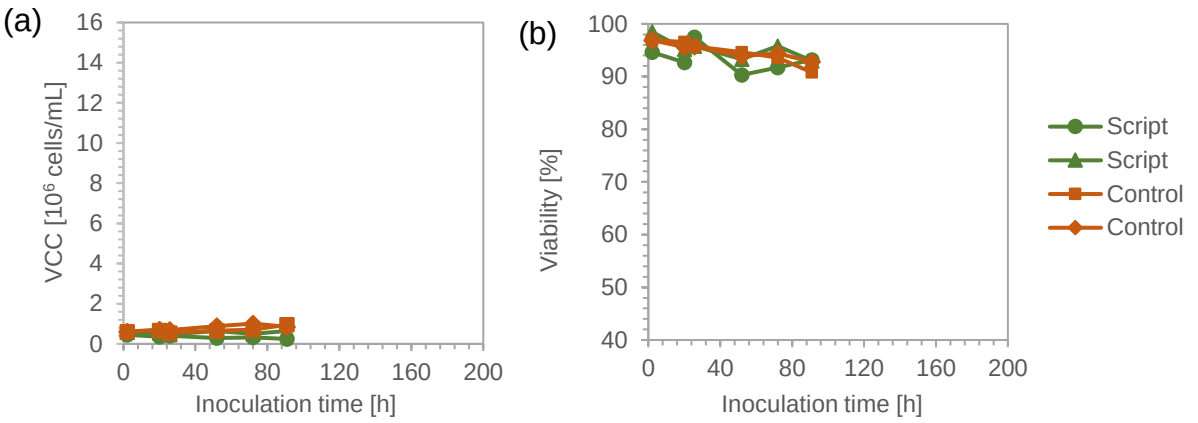

Figure 6: HEK293 fermentation processes with script application (green) and control (red) with (a) VCC [10^6 cells/mL] and (b) viability over inoculation time [h]; All fermentations were terminated after 90 h

Liste-Calleja et. al reported max. cell densities between 1 - 3×10^6 cells/mL in similar inoculation densities and a drastic increase by addition of Cell Boost 5 or FBS[138]. Other authors used inoculation densities of 0.8×10^6 cells/mL and observed max. cell densities of 6×10^6 cells/mL[139]. These examples do not yet confirm any hypothesis but provide a starting point for further inoculation studies. Also, sensitivity to shear stress has an influence on the cell growth[140,141]. Perfusion systems, in which higher cell densities were achieved, overcame this by milder aeration and agitation conditions[142].

Therefore, further optimization of process parameters in batch operation for successful HEK293 fermentations was crucial prior to implementation of the script which was beyond the scope of this work. Thus, HEK293 cells were not further investigated, but the initial testing of the developed soft sensor already gave some results on the necessary timeframes, oxygen PID control and data sampling frequency.

3.3 CHO fermentations

CHO cells were used as a second cell system to obtain robust fermentation processes and investigate implementation of the developed script for automated gas flow interruptions. Thus, the dynamic OUR can be measured in-situ and used for the development of the soft sensor by correlating the values to off-line determined VCC. Since negative impacts from gas flow interruption and changing %DO process values must be investigated, control processes without script application were included.

In total, two fermentation sets of CHO cells from two cryovials were performed, which led to triplicate processes with script application and control processes without script application. In the first fermentation, four vessels were used with half of the vessels with script application and control in the other half whereas in the second fermentation, two vessels were used for script application and control. All fermentations were successfully executed and resulted in max. cell densities of 9 - 15×10^6 cells/mL. After 160 h, all fermentations were terminated as

the viability declined to below 60%. Data plotting of cell densities and viabilities over the fermentation time did not reveal significant aberrations between the fermentations where the script was applied and the control. The variation between two fermentation sets exceeds the variation between script application and control vessels (Figure 7).

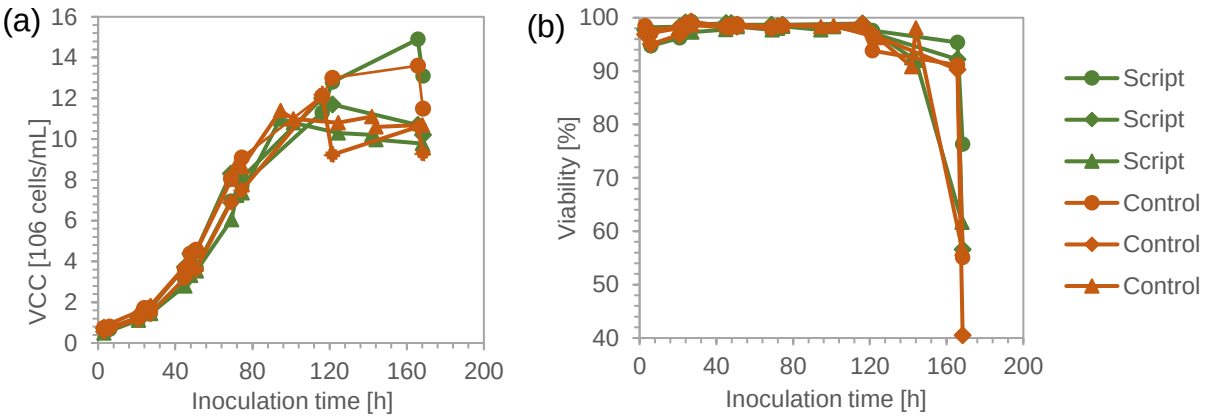

Figure 7: CHO fermentations with script application in process triplicates (green) and control in process triplicates (red) displaying (a) VCC [10^6 cells/mL] and (b) viability [%] over inoculation time [h]. Processes of the first fermentation are indicated by circle and rhombus marks, processes of second fermentation are indicated by triangle marks

The mAb titers of CHO fermentations were determined as previously described at day 7 after inoculation. In the first fermentation with four vessels, the mAb titers of script application processes exceeded the control processes by +4.3%. In the second fermentation, only two vessels were used, and the titres of the script application process deviated from the control processes by -26.4%. The processes result in a total deviation of 11.7% accompanied by a mean calibration error of 3.3%. Since positive and negative deviations were seen, no bias on the antibody titre productivity can be concluded.

3.4 Soft sensor development

The development of the soft sensor is based on process data from the previous fermentation process which leads to classification as data-driven soft sensor. In theory, the dynamic OUR increases with VCC and therefore, only these variables are necessary to include in the soft sensor model. While VCC can be measured off-line for dataset generation, the dynamic OUR can be determined by gas flow interruptions which were automated by the developed script in the control software of DASGIP® bioreactor system and applied in fermentation processes: Two sets of parallel fermentations of CHO cells led to a process triplicate and the dynamic OUR measurements offer the in-situ determined variable of the model which represents the measurable variable for soft sensor application. For development of the soft sensor, the following tasks have to be achieved: The dynamic OUR must be determined within measurements, the soft sensor model has to be assessed by statistical means and implementation of the soft sensor needs to be reasonable. Therefore, determination of

dynamic OUR based on stoic equations are made, the data sets are applied to statistical methods for model development and implementation of the soft sensor is investigated.

Dynamic OUR determination

Gas flow interruptions in the CHO fermentation processes were performed for dynamic OUR determinations with the goal of soft sensor development. For the model development itself, the methodology of dynamic OUR measurements, stoic equations and physical assumptions need to be applied. As an ultimate goal, the method should be justified according to scientific and engineering principles. Therefore, the cell specific oxygen consumption rates are considered and compared to literature values. The following approach of dynamic OUR determination refers directly to the output in the fermentation process with physical assumptions and calculational methods being discussed.

In the fermentation output, the aeration interruptions were automatically executed by the previously described script every 3 h and are exemplarily visualized in Figure 8. After the threshold of 30 %DO or a 10 min interval was reached and the gas flow was switched on again, the %DO further dropped afterwards depending on the viable cell concentration. In the selected timeframe in figure 8, the %DO dropped to app. 16% which results from the high oxygen demand of the rather high cell density of app. 9×10^6 cells/mL and the slow reacting nature of the PID controller for %DO. In this case, the %DO decline cannot be compensated within the first minutes of restarting the gas flow and therefore reasons the delay in reaching the %DO set point. In all gas flow interruptions, the %DO did not decline below 10% and therefore limitation of oxygen starvation is prevented. Further, the %DO drop at gas flow interruption lead to higher oscillation of %DO compared to Figure 5 of HEK293 fermentation. This is reasoned by higher cell densities in CHO fermentation (app. 9×10^6 cells/mL) compared to HEK293 (app. 0.7×10^6 cells/mL). Preferably, the %DO does not decrease below 50 %DO in the following regulation to prohibit negative influences on the cell growth at the development stage of the methodology. Reduced oxygen concentration has been reported to negatively influence the growth rate or lead to metabolism changes in *E. coli* and *Pichia pastoris*[143–145] which might also influence CHO cell growth to a lower extend, as the growth rate is much lower. The impact of the gas flow interruptions was therefore minimized by dynamic regulations. Further, 60 ± 5 %DO were reached before the gas flow interruption which was considered in %DO drop data generation. Consequently, the incomplete stabilization of %DO within 3 h was neglected in favor of more frequent data generation.

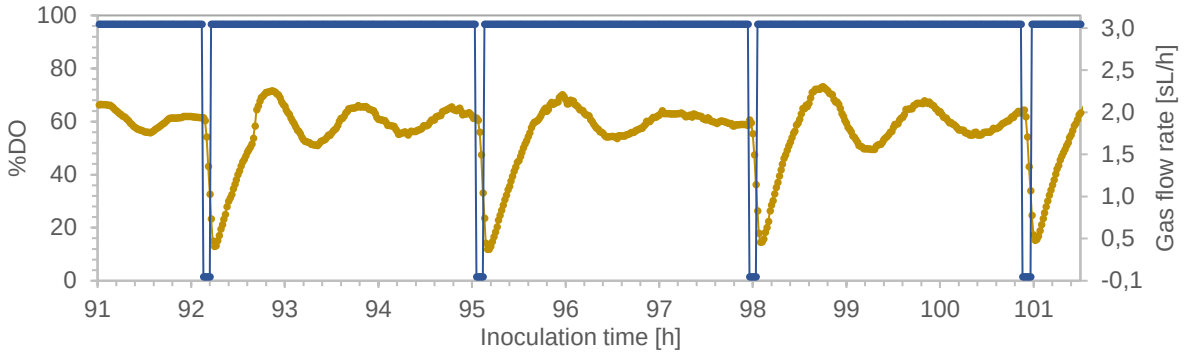

Figure 8: Script application in CHO fermentation with periodic gas flow interruption (black) and %DO regulation (gray) between 91-101.5 h inoculation time.

For dynamic OUR determination, oxygen balances are considered: In conventional aerated fermentation under steady-state condition, the oxygen transfer rate (OTR) is equal to OUR and is expressed by an extension of Equation 1 to

$$OUR = OTR = qO_2 * c_x = k_L a * \left(c_L{}^* - c_{O_2}\right)_{mean} \quad 2$$

with qO_2 specific oxygen uptake rate, c_x biomass concentration, $k_L a$ volumetric oxygen transfer coefficient, $c_L{}^*$ concentration of O_2 in liquid and in equilibrium with O_2 in air, c_{O_2} at measuring point in bioreactor. However, it has been discussed how $\left(c_L{}^* - c_{O_2}\right)_{mean}$ is used depending on mixing situation of gas bubbles[135]. Advantageously, the method of dynamic OUR determination avoids these difficulties and only requires the change of dissolved oxygen $\frac{dC}{dt}$ measured by the DO probe which simplifies in the non-gassing state to[135]

$$change\ in\ dissolved\ O_2\ concentration = OUR_{\ d} = qO_2 * c_x = \frac{dC}{dt} \quad 3$$

In the bioreactor, the concentration difference of dissolved oxygen is directly determined by

$$change\ in\ dissolved\ O_2\ concentration = \frac{d\%DO}{dt} = \frac{\%DO_{t_1} - \%DO_{t_2}}{t_2 - t_1} \quad 4$$

Therefore, the decline in every aeration stop was calculated by data sets with start ($\%DO_1$, t_1) and end points ($\%DO_2$, t_2) as indicated in **Fehler! Verweisquelle konnte nicht gefunden werden.**. The data was collected every 60 s which led to a respective uncertainty of %DO. As start point $\%DO_1$, t_1, the first data point where the flow rate was 0 sL/h was chosen. As end point $\%DO_2$, t_2, the first data point where the flow rate was again set to 3 sL/h was chosen. Linearity of the %DO drop between $\%DO_1$, t_1 and $\%DO_2$, t_2 was assumed. A short initial delay in %DO drop after gas flow interruption may be caused by an escape of hold-up air bubbles[135] and the first 60 s data collection timeframe is neglected in further calculations.

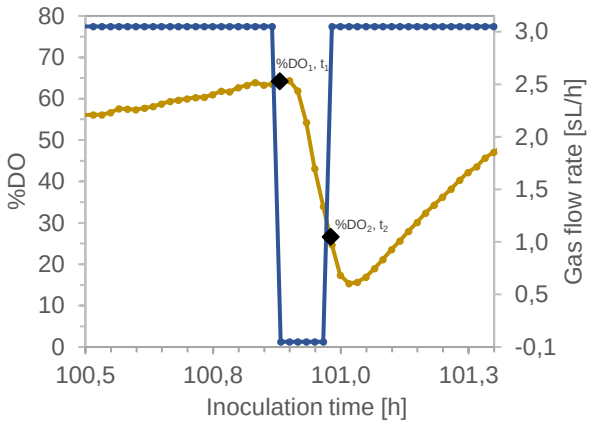

Figure 9: Gas flow interruption (blue) in CHO fermentation displaying start point %DO₁, t₁ (black) and end point %DO₂, t₂ (black) of %DO decline and linearity of decline (beige)

The change in dissolved oxygen concentration was determined for all gas flow interruptions. The decline of %DO per hour does not yield data comparable to the literature so further calculations to determine the dynamic OUR are made:

The typical ionic strength of mammalian cell culture media is 150 – 200 mM, resulting in 175 mM on average[146,147]. Henry's Law states that the molar concentration of dissolved gas $C_{(d)}$ [mM], is directly proportional to the partial pressure of the gas $P_{(g)}$ [mmHg] of the overlying air and the Henry constant H [mmHg/mM]:

$$C_{(d)} = P_{(g)}/H \qquad 5$$

The Henry constant for oxygen can be derived from experimental values at equilibrium of dissolved oxygen in air at different temperatures and ionic strengths[148] since direct measurements have not been available in literature so far. For mammalian cell culture medium at 37°C, 175 mM ionic strength, 100% humidity and neglecting 5% carbon dioxide, the dissolved oxygen concentration was extrapolated to 194 µmol/L[149]. The biggest influence on oxygen solubility is the temperature, which was kept constant in the experiments[149]. In a vessel of 600 mL media, the total amount dissolved oxygen is:

$$\frac{194 * 10^{-6}\, mol/L}{1000} * 600\, mL = 1.16 \times 10^{-4}\, mol \qquad 6$$

Since fermentations were operated at 60 %DO, the total dissolved oxygen in a vessel of 600 mL media is:

$$1.16 \times 10^{-4}\, mol * 0.6 = 6.98 \times 10^{-5}\, mol \qquad 7$$

6.98×10^{-5} mol implies the initial situation of 60 %DO in the fermentation, thus 1.16×10^{-6} mol correspond to 1 %DO. This enables multiplication with the %DO decline per hour (Equation 4)

to an oxygen consumption in mol O_2/h and further mol O_2/s. It has to be stated that varying units for specific oxygen consumption rates are found in literature e.g. mol/cell*h or amol/cell*s whereby amol refers to attomole or 10^{-18} mol. This thesis bases calculations on amol/cell*s.

Then, the respective cell densities are considered to determine the cell specific oxygen uptake rate per second qO_2 :

$$qO_2\,[amol\ O_2/\ cell * s] = \frac{mol\ O_2/s}{10^6\ viable\ cells/mL * 600\ mL * 10^{-18}} \qquad 8$$

The results are visualized in 10 and range between 9 - 19 amol O_2/cell*s. Although qO_2 is usually assumed as constant in bacterial processes, experiments proved otherwise[150] and come into agreement with the following observations in mammalian processes: In the exponential growth phase, qO_2 increases by high substrate consumption. After a maximum of qO_2 is reached, a decline follows. In Figure 10, insights on the qO_2 are given by depiction the data over the VCC in (a) and (b) for normalizing qO_2 to the VCC instead of inoculation time as well as depicting qO_2 over the inoculation time in (c). First, qO_2 increases slightly in all plots before a decline towards the end of the exponential growth phase can be seen in (a) and (b), indicated in all plots with a gray reference line. However, this behavior is not clearly indicated in (c), where the data is rather distributed and requires even deeper investigation.

In the further timeline, a pulse feed was applied at determined glucose concentrations below 3 g/L which extended the growth phase and increased qO_2 again. Subsequently, the feed was applied regularly which leads to flattening, but slightly oscillating behavior in (a) and (b) Towards higher cell densities, a decline of qO_2 is depicted as result of decreased metabolic activity[151] caused by substrate limitation and by-product formation[147]. In regard of the inoculation time in (c), a red line indicates the exponential growth phase on the left side, followed by the stationary growth phase where a non-oscillating decline is depicted.

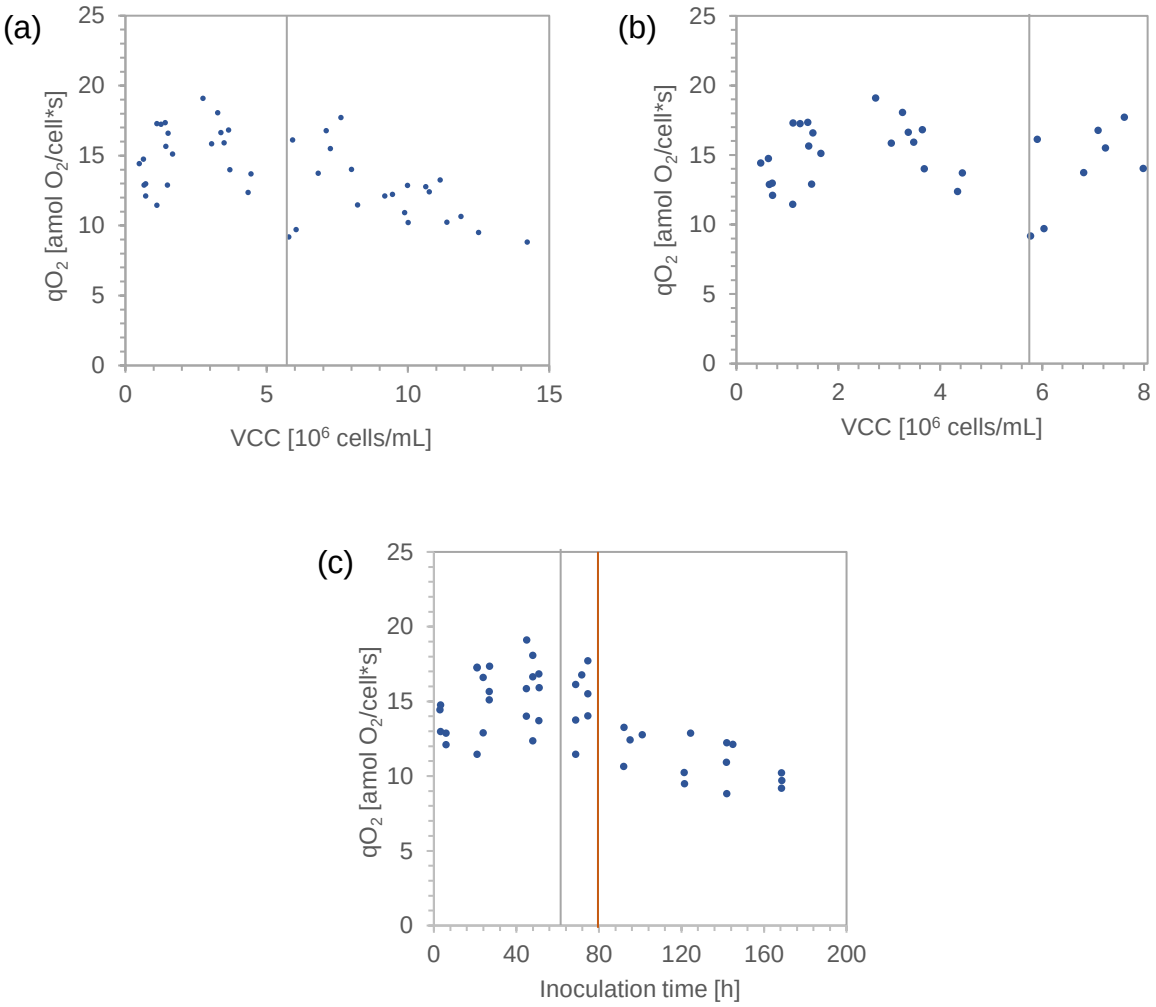

*Figure 10: Specific oxygen consumption rate qO_2 [amol O_2/cell*s] of CHO cells between (a) VCC 0-8×10^6 cells/mL, (b) VCC 0-15×10^6 cells/mL and (c) over inoculation time [t]*

The observations in Figure 10 (a) and (b) can be affirmed regarding the qO_2 peak in microbial processes in Figure 11 (a), proposed by Garcia-Ochoa et. al which behave similarly. Further, the previously determined dynamic OUR of all cells is displayed in Figure 11 (b) and strongly relates to a typic batch growth curve, with an extended stationary phase through the glucose feed. In Figure 10 (c), the end of the exponential growth phase is estimated at 80 h inoculation time which is also true for the OUR in Figure 11 (b).

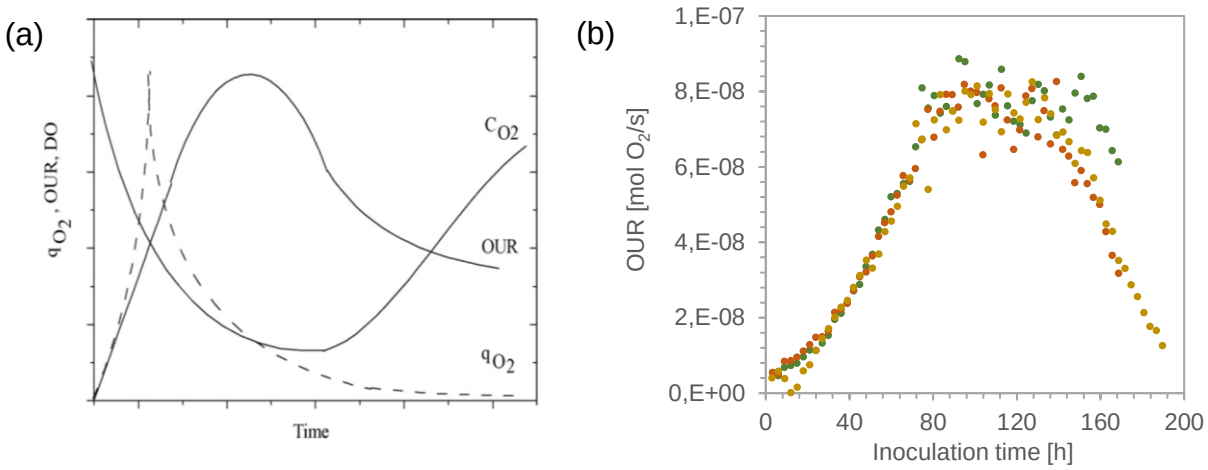

Figure 11: (a) Typical evolution of OUR, specific oxygen uptake rate qO_2 and DO concentration (cO_2) in time course of fermentation from Garcia-Ochoa et. al[151]; (b) dynamic OUR [mol O_2/s] over inoculation time [h] determined by process triplicates of CHO fermentations in red, green and beige

In literature, numerous papers dealing with qO_2 and its determination for CHO cells can be found which propose a range of 57.5 - 88 amol O_2/cell*s[149,152,153] whereas the dynamic measurement determined 9 - 19 amol O_2/cell*s. Up to 50% underestimations of dynamic OUR have been reported and are referred to the 'cellular economy principle' for which microorganisms consume oxygen at a lower rate during interrupted oxygen transfer[151,154,155]. Also, technical aberrations may be given by oxygen transfer from head space into liquid phase which could be overcome by sparging N_2 in the headspace[135].

However, the variation of VCC over the inoculation time in the literature seems to exceed the variation of qO_2 values in our experiments. For the sake of simplification, the assumptions of other authors[135,156] are accepted and qO_2 is assumed to be constant in the following model development.

Model development

From previous dynamic OUR measurements and investigations in the methodology, off-line determined VCC from the CHO fermentations are now considered for development of the soft sensor model. The hypothesis of increasing oxygen consumption by increasing VCC is now tested by finding a statistic reasonable correlation. Also, the coverage of the model on fermentation phases is investigated by statistical means. The generated data sets are applied to assumed linear regression models with the OUR as variable X predicting viable cell count as quantitative response Y in Microsoft Excel and R Studio.

The model is visualized in Figure 12 and displays the complete data set with the dynamic OUR and VCC up to 14×10^6 cells/mL of CHO fermentation processes. The trend line can be described as:

$$y = 1E + 08x - 0.3815$$

The negative intercept, which is something that is physically implausible is due to the increasing data variance with higher cell concentrations. The determination coefficient R^2 of 0.8907 describes the explained variance from data to model. Although R^2 of 0.8907 can be considered as valid linear regression, increased data variance beyond a VCC of 8×10^6 cells/mL can be seen. This is accompanied by the end of the exponential cell growth phase in the fermentation experiments.

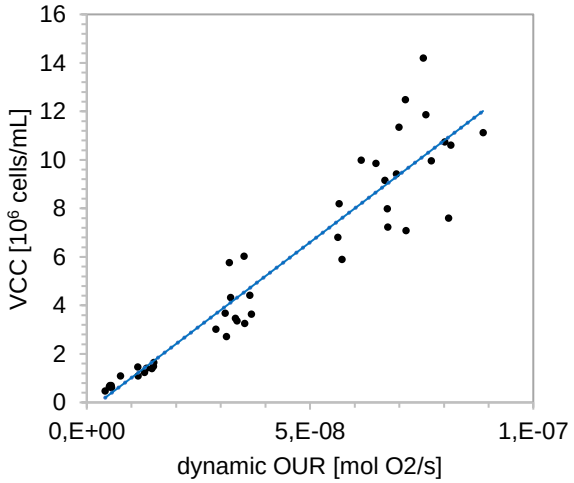

Figure 12: Soft sensor model thorough CHO cell fermentation up to 14×10^6 cells/mL

The model is improved by limiting the linear area to the exponential cell growth phase, which corresponds to a cell concentration of up to 8×10^6 cells/mL (Figure 13). The trend line in the adapted model is:

$$y = 1E + 08x + 0.1064$$

The positive intercept leaves a variance of 0.1064×10^6 cells/mL for which OUR could not be considered. The R^2 of 0.9693 shows a good model fit.

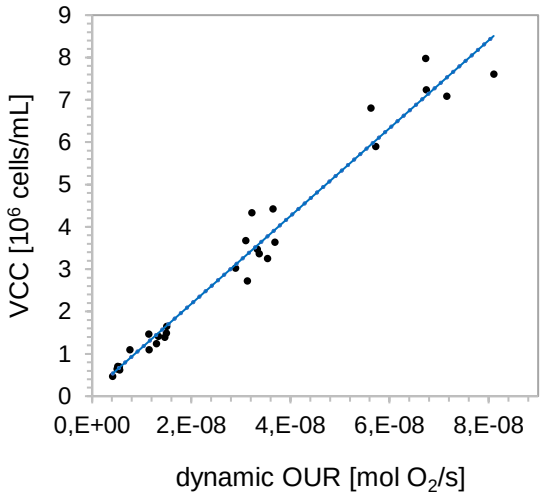

Figure 13: Soft sensor model in exponential growth phase of CHO cells up to *8×10^6 cells/mL*

A regular data collection would improve the correlations as more time points would be added and the whole linear area could be described. Nonetheless, a strong and traceable linear regression could be established.

Further statistical analysis was performed in R studio: The soft sensor with a confidence interval of 0.95 is displayed in Figure 14. Therefore, repeated measurements will lie in the confidence interval with a probability of 95%. Optimization of the model is feasible by incorporation of more data sets which narrows the confidence interval, but the confidence interval is tight enough for the use as an online soft sensor.

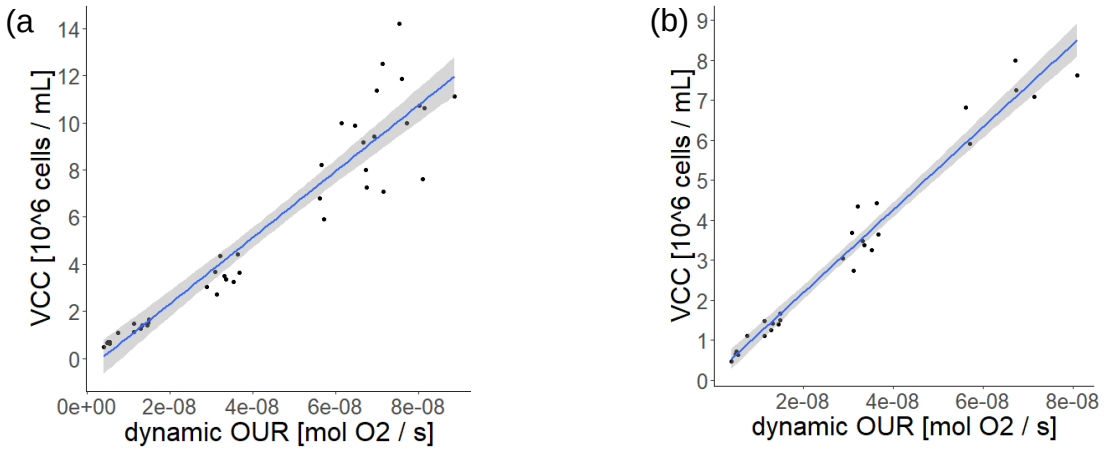

Figure 14: Soft sensor for determining VCC [10^6 cells/mL] by dynamic OUR [mol O2/s] with linear soft sensor model (blue), based on data sets (black) and confidence interval (gray) in (a) in the exponential growth phase up to 8×10^6 cells/mL and (b) 14×10^6 cells/mL of CHO cells

In this analysis, application of the linear model in the exponential growth phase of CHO cells until 8×10^6 cells/mL is suggested by the determination coefficient of 0.9693 and narrowed confidence interval. This may be reflected by the specific oxygen consumption rates qO_2 results in Figure 10 as qO_2 may decline in the stationary cell growth phase. For specific interest and

application in the stationary cell growth phase, the declining qO_2 may be incorporated in a two-segmented model.

Soft sensor implementation

The proposed model was implemented to predict the VCC by in-situ determined dynamic OUR to complete the soft sensor development. For successful application, the soft sensor needs to be robust and precise which will be tested by retrospective validation on previous fermentation process.

The proposed linear model was applied to each single run of CHO fermentation separately. Tthe validation is only assumed to be valid below VCC of 8×10^6 cells/mL as discussed before. The soft sensor is visualized in comparison to the actual processes in Figure 15. A strong agreement is given between soft sensor and offline measurements. Only the validation in Figure 15 (b) shows slight aberration in the soft sensor but the following off-line VCC declined as well. This may suggest one extraordinary high VCC was measured by imprecise sampling, something that the soft sensor is not suffering from. In (c), an initial decline is given which results from an incorrectly installed DO probe. Overall, it can be pointed out that the soft sensor offers by far more VCC data points as dynamic OUR measurements were performed every 3 h whereas off-line VCC in mammalian cell culture is typically performed only once or twice a day. It also shows that the soft sensor is not suffering from any sampling deviations.

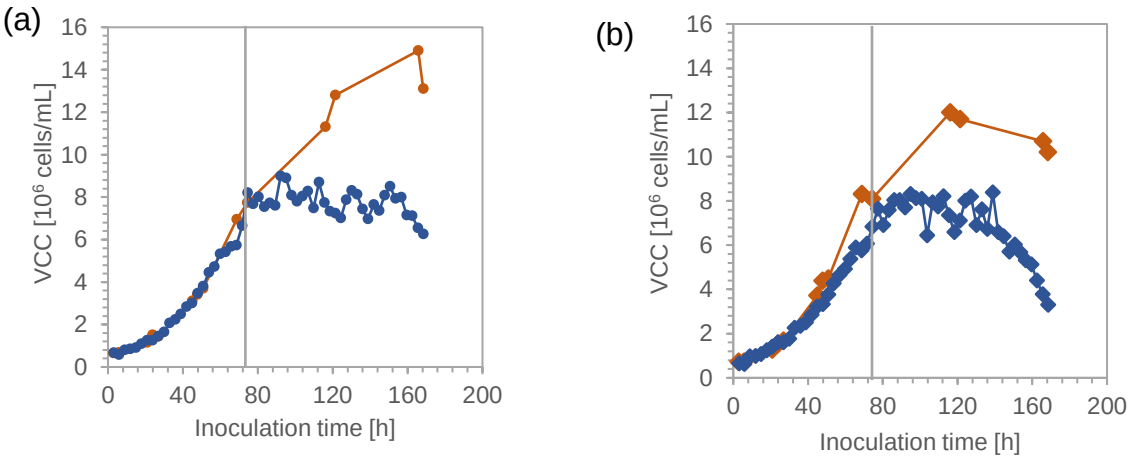

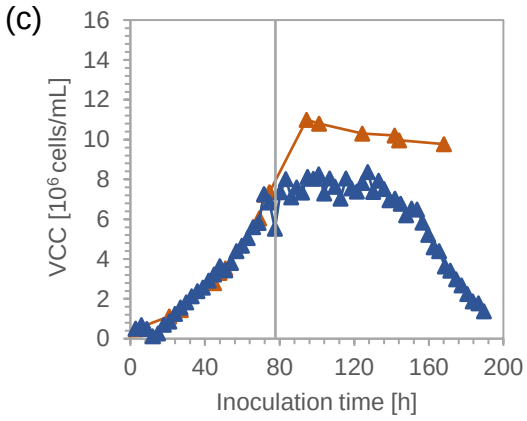

Figure 15: Implementation of soft sensor in process triplicates over inoculation time [h] with soft sensor prediction (blue) and reference processes (red) in three processes (a), (b), (c) in exponential growth phase of CHO cells up to 8×10⁶ cells/mL, indicated by reference line

3.5 Tn*ms*42 fermentations

The transferability of the soft sensor model from CHO cells to the insect cell line Tn*ms*42 was studied to assess the application of the soft sensor in another cell system. Subsequently, certain parameters had to be adapted, the soft sensor methodology followed and especially the soft sensor model needs to be found again.

The transferability of the method required adaptation in the standard gas flow rate from 3 sL/h to 0.3 sL/h whereas other parameters in the script application were kept constant. Further differences between the cell systems were derived from established fermentation parameters e.g. stirrer speed and pH control. Different passaging numbers for two Tn*ms*42 fermentations were taken. Therefore, two fermentations of Tn*ms*42 cells were performed which led to three vessels with script application and two control vessels without script application. The first Tn*ms*42 fermentation resulted in maximum cell densities of 8 – 10.5×10^6 cells/mL whereby the VCCs in vessels with script were reported slightly higher than the control vessel without script. Thus, negative influences of aeration interruption on growth parameter are excluded which was equally reported by Wong et. al in Sf9 cells[157]. Termination of the fermentations after 96 h was caused by a general oxygen flow defect.

The second Tn*ms*42 fermentation was aborted already at 27 h due to a fungal contamination and could not be considered in further calculations. All processes are depicted in Figure 16.

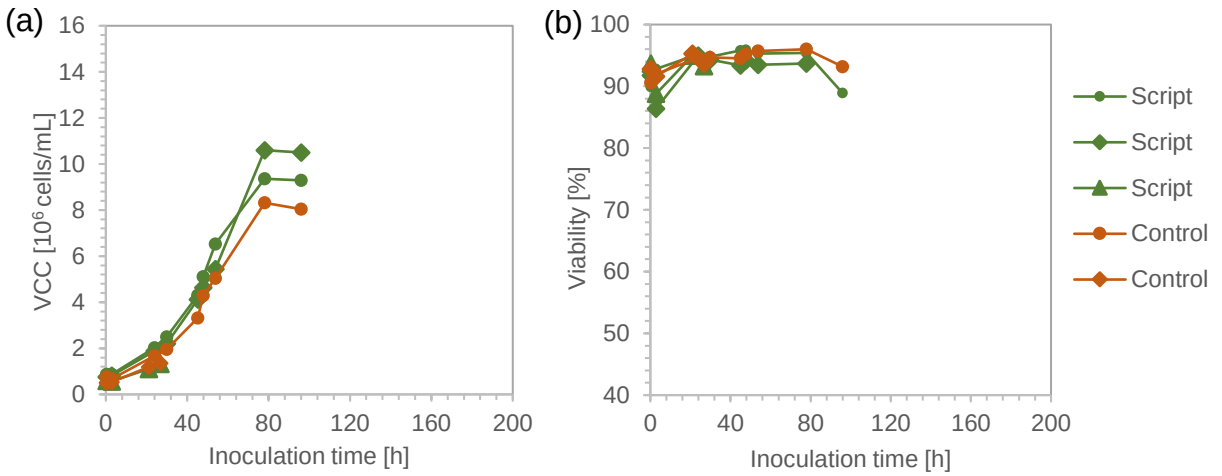

Figure 16: Tnms42 fermentations with script application in three processes (green) and two control processes (red) displaying (a) VCC [10^6 cells/mL] and (b) viability [%] over inoculation time [h]

The dynamic OUR and qO_2 determination were performed as previously described and are depicted in Figure 17. Most qO_2 values are varying between 0.8 – 6 amol O_2/s. However, two extra ordinary high qO_2 values (19 amol O_2/s and 22 amol O_2/s) were measured which cannot be related to the previously described qO_2 peaks at the exponential growth phase end in mammalian cell culture and bacterial fermentation (Figure 17 (a)). This phenomenon is also reflected in Figure 17 (b). Furthermore, no sigmoid behavior can be observed compared to Figure 11 (b). The dynamic OUR and off-line determined VCC were plotted for further investigation but as indicated in Figure 17 (c), no correlation can be obtained.

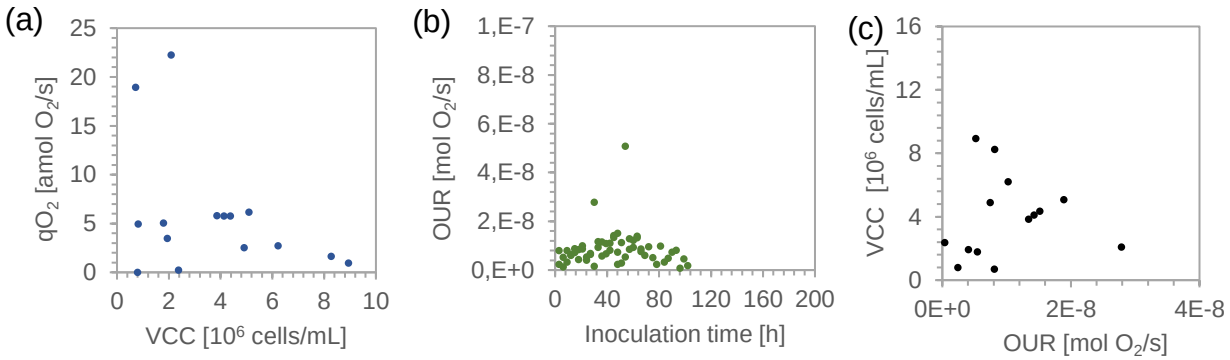

Figure 17: Tnms42 evaluation (a) qO_2 [amol O_2/s] over VCC [10^6 cells/mL] (b) OUR [mol O_2/s] over inoculation time [h] (c) VCC [10^6 cells/mL] and OUR [mol O_2/s] plot

In literature, qO_2 values of High Five™ cells begin with 100 amol O_2/s and even a deduction of 50% would lead to qO_2 of at least 50 amol O_2/s. Wong et. al suggested the k_La is not negligible for rather low fermentation volumes and especially not at high stirrer speed. Therefore, it could be hypothesized that the increased stirrer speed of 200 rpm favored oxygen transfer from headspace to liquid phase. These insights offer a starting point for future transfer of the soft sensor in insect cells and point directly to usage of lower headspace volume by higher fermentation volumes, varying k_La and lower stirrer speed if applicable.

4. Conclusion

Automated and repetitive gas flow interruptions for dynamic OUR measurements in CHO cells were successfully realized through elaborate script development. The conversion and application of the measured values were performed by deriving the oxygen solubility in the media and neglecting $k_L a$ in the non-gassing state. Further insights into the specific oxygen uptake rate qO_2 were gained, underlining earlier assumptions from the literature that these are not thoroughly constant throughout the fermentation process. In addition, the qO_2 values were lower than those reported in the literature, whereby a 50% deviation was caused by the method itself. Further deviations may be assumed to adapt to cell respiration under aeration interruption or the influence of $k_L a$ from the headspace. A major advantage of the dynamic OUR is that these apparent values are both sufficient and specific. Using dynamic OUR values and off-line determined viable cell counts, the soft sensor model was established and statistically investigated in different process phases. The soft sensor provided an excellent fit in the exponential growth phase of CHO cells, despite neglecting the non-constant specific oxygen uptake rate, which underlines the robustness of the method.

Overall cell systems used, no negative influences or significant aberrations on growth rate, maximum cell density, viability and mAb production of CHO cells were observed. Although transferability to Tn*ms*42 cells was not successful, studies on $k_L a$, stirrer speed, fermentation volume and headspace volume may reveal further information.

In the future, this on-line, in-situ soft sensor may be further developed to real-time application which is feasible by implementing the linear model into the script and using real-time %DO process values. Therefore, 24 more internal values and notifications within DASware® offer building blocks. For prospective applications, the model may be refined by additional data sets since those will narrow the confidence interval of the model. Thereby, the prediction can be sophisticated, and this model may be further validated for prospective applications.

Soft sensors are promising tools for PAT, combine heightened bioprocess understanding and sophisticated modelling concepts, and may finally close the gap to QbD. This thesis proposed a soft sensor for simplified viable cell counting which in-situ application and prospective real-time prediction are following the right track to implementation of PAT principles.

References

1. Woodcock, J. & Woosley, R. The FDA Critical Path Initiative and Its Influence on New Drug Development. *Annu Rev Med* **59**, 1–12 (2008).

2. Scannell, J. W., Blanckley, A., Boldon, H. & Warrington, B. Diagnosing the decline in pharmaceutical R&D efficiency. *Nat Rev Drug Discov* **11**, 191–200 (2012).

3. Berkowitz BA. Basic and Clinical Pharmacology. in *11th ed. New Delhi: Tata McGraw Hill* (eds. Katzung, B., Masters, S. & Trevor, A.) 67 (2009).

4. Paul, S. M. *et al.* How to improve R&D productivity: the pharmaceutical industry's grand challenge. *Nat Rev Drug Discov* **9**, 203–214 (2010).

5. Mahajan, R. & Gupta, K. Food and drug administration′s critical path initiative and innovations in drug development paradigm: Challenges, progress, and controversies. *J Pharm Bioallied Sci* **2**, 307 (2010).

6. Munos, B. Lessons from 60 years of pharmaceutical innovation. *Nat Rev Drug Discov* **8**, 959–968 (2009).

7. Grilo, A. L. & Mantalaris, A. The Increasingly Human and Profitable Monoclonal Antibody Market. *Trends Biotechnol* **37**, 9–16 (2019).

8. Kessel, M. The problems with today's pharmaceutical business—an outsider's view. *Nat Biotechnol* **29**, 27–33 (2011).

9. Farid, S. S., Baron, M., Stamatis, C., Nie, W. & Coffman, J. Benchmarking biopharmaceutical process development and manufacturing cost contributions to R&D. *MAbs* **12**, (2020).

10. U.S. Department of Health and Human Services Food and Drug Administration. *Innovation or Stagnation: Challenge and Opportunity on the Critical Path to New Medical Products*. (2004).

11. Rolinger, L., Rüdt, M. & Hubbuch, J. A critical review of recent trends, and a future perspective of optical spectroscopy as PAT in biopharmaceutical downstream processing. *Anal Bioanal Chem* **412**, 2047–2064 (2020).

12. Streefland, M., Martens, D. E., Beuvery, E. C. & Wijffels, R. H. Process analytical technology (PAT) tools for the cultivation step in biopharmaceutical production. *Eng Life Sci* **13**, 212–223 (2013).

13. U.S. Food and Drug Administration. PAT — A Framework for Innovative Pharmaceutical Development, Manufacturing, and Quality Assurance . *https://www.fda.gov/regulatory-information/search-fda-guidance-documents/pat-framework-innovative-pharmaceutical-development-manufacturing-and-quality-assurance* (2004).

14. Eon-Duval, A., Broly, H. & Gleixner, R. Quality attributes of recombinant therapeutic proteins: An assessment of impact on safety and efficacy as part of a quality by design development approach. *Biotechnol Prog* **28**, 608–622 (2012).

15. Mishra, V., Thakur, S., Patil, A. & Shukla, A. Quality by design (QbD) approaches in current pharmaceutical set-up. *Expert Opinion on Drug Delivery* vol. 15 737–758 Preprint at https://doi.org/10.1080/17425247.2018.1504768 (2018).

16. Reklaitis, G. v., Khinast, J. & Muzzio, F. Pharmaceutical engineering science—New approaches to pharmaceutical development and manufacturing. *Chemical Engineering Science* vol. 65 iv–vii Preprint at https://doi.org/10.1016/j.ces.2010.08.041 (2010).

17. Rantanen, J. & Khinast, J. The Future of Pharmaceutical Manufacturing Sciences. *J Pharm Sci* **104**, 3612–3638 (2015).

18. Collins, F. S. & Varmus, H. A New Initiative on Precision Medicine. *New England Journal of Medicine* **372**, 793–795 (2015).

19. Ayati, N., Saiyarsarai, P. & Nikfar, S. Short and long term impacts of COVID-19 on the pharmaceutical sector. (2020) doi:10.1007/s40199-020-00358-5/Published.

20. Kelley, B. Developing therapeutic monoclonal antibodies at pandemic pace. *Nat Biotechnol* **38**, 540–545 (2020).

21. Tuccori, M. *et al.* Anti-SARS-CoV-2 neutralizing monoclonal antibodies: clinical pipeline. *MAbs* **12**, (2020).

22. Mishra, V., Thakur, S., Patil, A. & Shukla, A. Quality by design (QbD) approaches in current pharmaceutical set-up. *Expert Opinion on Drug Delivery* vol. 15 737–758 Preprint at https://doi.org/10.1080/17425247.2018.1504768 (2018).

23. International Conference on Harmonisation of Technical Requirements for Registration of Pharmaceuticals for Human Use. Pharmaceutical Development Q8(R2). *https://www.ich.org/page/quality-guidelines* (2009).

24. International Conference on Harmonisation of Technical Requirements for Registration of Pharmaceuticals for Human Use. Quality Risk Management Q9. *https://www.ich.org/page/quality-guidelines* (2005).

25. International Conference on Harmonisation of Technical Requirements for Registration of Pharmaceuticals for Human Use. Pharmaceutical Quality Systems (Q10). *https://www.ich.org/page/quality-guidelines* (2008).

26. International Conference on Harmonisation of Technical Requirements for Registration of Pharmaceuticals for Human Use. Development and Manufacture of Drug Substances (Chemical Entities and Biotechnological/Biological Entities) (Q11). *https://www.ich.org/page/quality-guidelines* (2012).

27. Aksu, B. *et al.* Strategic funding priorities in the pharmaceutical sciences allied to Quality by Design (QbD) and Process Analytical Technology (PAT). *European Journal of Pharmaceutical Sciences* vol. 47 402–405 Preprint at https://doi.org/10.1016/j.ejps.2012.06.009 (2012).

28. Rathore, A. S. Roadmap for implementation of quality by design (QbD) for biotechnology products. *Trends in Biotechnology* vol. 27 546–553 Preprint at https://doi.org/10.1016/j.tibtech.2009.06.006 (2009).

29. McMahon, T. & Wright, E. L. *Analytical Instrumentation: A Practical Guide for Measurement and Control*. (Instrument Society of America: Research Triangle Park, NC, , 1996).

30. Workman, J., Koch, M., Lavine, B. & Chrisman, R. Process Analytical Chemistry. *Anal Chem* **81**, 4623–4643 (2009).

31. Callis, J. B., Illman, D. L. & Kowalski, B. R. Process analytical chemistry. *Anal Chem* **59**, 624A-637A (1987).

32. Yu, L. X. *et al.* Understanding pharmaceutical quality by design. *AAPS Journal* vol. 16 771–783 Preprint at https://doi.org/10.1208/s12248-014-9598-3 (2014).

33. Rathore A. S. & Winkle H. Quality by Design for Biopharmaceuticals. *Nature Biotechnology* **27**, 26–34 (2009).

34. Nishendu P. Nadpara. QBD review. *Int. J Pharm Sci Rev Res* **4**, 20–28 (2012).

35. Sommeregger, W. *et al.* Quality by control: Towards model predictive control of mammalian cell culture bioprocesses. *Biotechnology Journal* vol. 12 Preprint at https://doi.org/10.1002/biot.201600546 (2017).

36. Challener, C. A. Moving PAT from Concept to Reality. *BioPharm International* (2019).

37. CMC Biotech Working Group. A-Mab: A Case Study in Bioprocess Development. Preprint at (2009).

38. Martin-Moe, S. & Nast, C. An Overview of Quality by Design for Drug Product. in 47–59 (2015). doi:10.1007/978-1-4939-2316-8_4.

39. Pais, D. A. M., Carrondo, M. J. T., Alves, P. M. & Teixeira, A. P. Towards real-time monitoring of therapeutic protein quality in mammalian cell processes. *Current Opinion in Biotechnology* vol. 30 161–167 Preprint at https://doi.org/10.1016/j.copbio.2014.06.019 (2014).

40. Konstantinov, K. B. & Cooney, C. L. White paper on continuous bioprocessing May 20-21, 2014 continuous manufacturing symposium. *Journal of Pharmaceutical Sciences* vol. 104 813–820 Preprint at https://doi.org/10.1002/jps.24268 (2015).

41. Nepveux, K., Sherlock, J.-P., Futran, M., Thien, M. & Krumme, M. How Development and Manufacturing Will Need to Be Structured—Heads of Development/Manufacturing May 20–21, 2014 Continuous Manufacturing Symposium. *J Pharm Sci* **104**, 850–864 (2015).

42. Warikoo, V. *et al.* Integrated continuous production of recombinant therapeutic proteins. *Biotechnol Bioeng* **109**, 3018–3029 (2012).

43. Simon, L. L. *et al.* Assessment of Recent Process Analytical Technology (PAT) Trends: A Multiauthor Review. *Org Process Res Dev* **19**, 3–62 (2015).

44. Luttmann, R. *et al.* Soft sensors in bioprocessing: A status report and recommendations. *Biotechnology Journal* vol. 7 1040–1048 Preprint at https://doi.org/10.1002/biot.201100506 (2012).

45. Kadlec P, Gabrys B & Strandt S. Data-driven soft sensors in the process industry. *Comput. Chem. Eng.* **33**, 795–814 (2009).

46. Paulsson, D., Gustavsson, R. & Mandenius, C. F. A soft sensor for bioprocess control based on sequential filtering of metabolic heat signals. *Sensors (Switzerland)* **14**, 17864–17882 (2014).

47. Mandenius, C.-F. & Gustavsson, R. Mini-review: soft sensors as means for PAT in the manufacture of bio-therapeutics. *Journal of Chemical Technology & Biotechnology* **90**, 215–227 (2015).

48. Grangeia, H. B., Silva, C., Simões, S. P. & Reis, M. S. Quality by design in pharmaceutical manufacturing: A systematic review of current status, challenges and future perspectives. *European Journal of Pharmaceutics and Biopharmaceutics* **147**, 19–37 (2020).

49. Deloitte. 2020 Global life sciences outlook. *https://www2.deloitte.com/global/en/pages/life-sciences-and-healthcare/articles/global-life-sciences-sector-outlook.html.* (2020).

50. Lu, R. M. *et al.* Development of therapeutic antibodies for the treatment of diseases. *Journal of Biomedical Science* vol. 27 Preprint at https://doi.org/10.1186/s12929-019-0592-z (2020).

51. Garattini, L. & Padula, A. Precision medicine and monoclonal antibodies: Breach of promise? *Croatian Medical Journal* vol. 60 284–289 Preprint at https://doi.org/10.3325/cmj.2019.60.284 (2019).

52. Singh, S. *et al.* Monoclonal Antibodies: A Review. *Curr Clin Pharmacol* **13**, 85–99 (2018).

53. Kaplon, H., Chenoweth, A., Crescioli, S. & Reichert, J. M. Antibodies to watch in 2022. *MAbs* **14**, (2022).

54. Hong, M. S. *et al.* Challenges and opportunities in biopharmaceutical manufacturing control. *Computers and Chemical Engineering* vol. 110 106–114 Preprint at https://doi.org/10.1016/j.compchemeng.2017.12.007 (2018).

55. Ecker, D. M., Jones, S. D. & Levine, H. L. The therapeutic monoclonal antibody market. *MAbs* **7**, 9–14 (2015).

56. O'Flaherty, R. *et al.* Mammalian cell culture for production of recombinant proteins: A review of the critical steps in their biomanufacturing. *Biotechnol Adv* **43**, 107552 (2020).

57. Birch, J. R. & Racher, A. J. Antibody production. *Adv Drug Deliv Rev* **58**, 671–685 (2006).

58. Lalonde, M.-E. & Durocher, Y. Therapeutic glycoprotein production in mammalian cells. *J Biotechnol* **251**, 128–140 (2017).

59. Durocher, Y. & Butler, M. Expression systems for therapeutic glycoprotein production. *Curr Opin Biotechnol* **20**, 700–707 (2009).

60. Walsh G. Post-translational modifications of protein biopharmaceuticals. *Drug Discov. Today* **15**, 773–780.

61. Rozov, S. M., Permyakova, N. v. & Deineko, E. v. Main Strategies of Plant Expression System Glycoengineering for Producing Humanized Recombinant Pharmaceutical Proteins. *Biochemistry (Moscow)* **83**, 215–232 (2018).

62. Clark, D. P. & Pazdernik, N. J. Protein Synthesis. in *Molecular Biology* e250–e255 (Elsevier, 2013). doi:10.1016/B978-0-12-378594-7.00047-0.

63. Huang, Y.-M. *et al.* Maximizing productivity of CHO cell-based fed-batch culture using chemically defined media conditions and typical manufacturing equipment. *Biotechnol Prog* **26**, 1400–1410 (2010).

64. Huang, Z. *et al.* Insights into the Impact of Rosmarinic Acid on CHO Cell Culture Improvement through Transcriptomics Analysis. *Processes* **10**, (2022).

65. Huang, Z. *et al.* Insights into the Impact of Rosmarinic Acid on CHO Cell Culture Improvement through Transcriptomics Analysis. *Processes* **10**, 533 (2022).

66. Arena, T. A., Chou, B., Harms, P. D. & Wong, A. W. An anti-apoptotic HEK293 cell line provides a robust and high titer platform for transient protein expression in bioreactors. *MAbs* **11**, 977–986 (2019).

67. Bandaranayake, A. D. & Almo, S. C. Recent advances in mammalian protein production. *FEBS Lett* **588**, 253–260 (2014).

68. Jayapal, K. & Wlaschin, K. Recombinant protein therapeutics from CHO cells-20 years and counting. *Chem. Eng. Prog.* **103**, 40–47.

69. Jadhav, V. *et al.* CHO microRNA engineering is growing up: Recent successes and future challenges. *Biotechnol Adv* **31**, 1501–1513 (2013).

70. Urlaub, G. & Chasin, L. A. Isolation of Chinese hamster cell mutants deficient in dihydrofolate reductase activity. *Proceedings of the National Academy of Sciences* **77**, 4216–4220 (1980).

71. Russell, W. C., Graham, F. L., Smiley, J. & Nairn, R. Characteristics of a Human Cell Line Transformed by DNA from Human Adenovirus Type 5. *Journal of General Virology* **36**, 59–72 (1977).

72. Graham, F. L. Growth of 293 Cells in Suspension Culture. *Journal of General Virology* **68**, 937–940 (1987).

73. Garnier, A., Côté, J., Nadeau, I., Kamen, A. & Massie, B. Scale-up of the adenovirus expression system for the production of recombinant protein in human 293S cells. *Cytotechnology* **15**, 145–155 (1994).

74. DuBridge, R. B. *et al.* Analysis of mutation in human cells by using an Epstein-Barr virus shuttle system. *Mol Cell Biol* **7**, 379–387 (1987).

75. Durocher, Y. High-level and high-throughput recombinant protein production by transient transfection of suspension-growing human 293-EBNA1 cells. *Nucleic Acids Res* **30**, 9e–99 (2002).

76. Walsh, G. Post-translational modifications of protein biopharmaceuticals. *Drug Discov Today* **15**, 773–780 (2010).

77. Backliwal, G. *et al.* Rational vector design and multi-pathway modulation of HEK293E cells yield recombinant antibody titers exceeding 1 g/l by transient transfection under serum-free conditions. *Nucleic Acids Res* **36**, e96–e96 (2008).

78. Backliwal, G. *et al.* Rational vector design and multi-pathway modulation of HEK293E cells yield recombinant antibody titers exceeding 1 g/l by transient transfection under serum-free conditions. *Nucleic Acids Res* **36**, e96–e96 (2008).

79. Ikonomou, L., Schneider, Y.-J. & Agathos, S. N. Insect cell culture for industrial production of recombinant proteins. *Appl Microbiol Biotechnol* **62**, 1–20 (2003).

80. Bédard, C., Kamen, A., Tom, R. & Massie, B. Maximization of recombinant protein yield in the insect cell/baculovirus system by one-time addition of nutrients to high-density batch cultures. *Cytotechnology* **15**, 129–138 (1994).

81. Tapia, F., Vázquez-Ramírez, D., Genzel, Y. & Reichl, U. Bioreactors for high cell density and continuous multi-stage cultivations: options for process intensification in cell culture-based viral vaccine production. *Appl Microbiol Biotechnol* **100**, 2121–2132 (2016).

82. Krammer, F. *et al.* Trichoplusia ni cells (High FiveTM) are highly efficient for the production of influenza A virus-like particles: a comparison of two insect cell lines as production platforms for influenza vaccines. *Mol Biotechnol* **45**, 226–234 (2010).

83. Harrison, R. L. & Jarvis, D. L. Protein N-Glycosylation in the Baculovirus–Insect Cell Expression System and Engineering of Insect Cells to Produce "Mammalianized" Recombinant Glycoproteins. in 159–191 (2006). doi:10.1016/S0065-3527(06)68005-6.

84. Wickham, T. J., Davis, T., Granados, R. R., Shuler, M. L. & Wood, H. A. Screening of insect cell lines for the production of recombinant proteins and infectious virus in the baculovirus expression system. *Biotechnol Prog* **8**, 391–396 (1992).

85. Chen, Y.-R. *et al.* The Transcriptome of the Baculovirus Autographa californica Multiple Nucleopolyhedrovirus in Trichoplusia ni Cells. *J Virol* **87**, 6391–6405 (2013).

86. Chen, Y.-R. *et al.* Transcriptome Responses of the Host Trichoplusia ni to Infection by the Baculovirus Autographa californica Multiple Nucleopolyhedrovirus. *J Virol* **88**, 13781–13797 (2014).

87. Granados, R. R., Guoxun, L., Derksen, A. C. G. & McKenna, K. A. A new insect cell line from Trichoplusia ni (BTI-Tn-5B1-4) susceptible to Trichoplusia ni single enveloped nuclear polyhedrosis virus. *J Invertebr Pathol* **64**, 260–266 (1994).

88. Wickham, T. J. & Nemerow, G. R. Optimization of growth methods and recombinant protein production in BTI-Tn-5B1-4 insect cells using the baculovirus expression system. *Biotechnol Prog* **9**, 25–30 (1993).

89. Koczka, K. *et al.* Comparative transcriptome analysis of a Trichoplusia ni cell line reveals distinct host responses to intracellular and secreted protein products expressed by recombinant baculoviruses. *J Biotechnol* **270**, 61–69 (2018).

90. Geisler, C. & Jarvis, D. L. Adventitious viruses in insect cell lines used for recombinant protein expression. *Protein Expr Purif* **144**, 25–32 (2018).

91. Maghodia, A. B., Geisler, C. & Jarvis, D. L. A new nodavirus-negative Trichoplusia ni cell line for baculovirus-mediated protein production. *Biotechnol Bioeng* **117**, 3248–3264 (2020).

92. Kiviharju, K., Salonen, K., Moilanen, U. & Eerikäinen, T. Biomass measurement online: the performance of in situ measurements and software sensors. *J Ind Microbiol Biotechnol* **35**, 657–665 (2008).

93. Olsson, L. & Nielsen, J. On-line and in situ monitoring of biomass in submerged cultivations. *Trends Biotechnol* **15**, 517–522 (1997).

94. Davey, C. L. & Kell, D. B. The influence of electrode polarisation on dielectric spectra, with special reference to capacitive biomass measurements: II/ Reduction in the contribution of electrode polarisation to dielectric spectra using a two-frequency method. *Bioelectrochemistry and Bioenergetics* **46**, 105–114 (1998).

95. Marose, S. Optical sensor systems for bioprocess monitoring. *Trends Biotechnol* **17**, 30–34 (1999).

96. Zhang, H. & Lennox, B. Integrated condition monitoring and control of fed-batch fermentation processes. *J Process Control* **14**, 41–50 (2004).

97. Markx, G. H. & Davey, C. L. The dielectric properties of biological cells at radiofrequencies: applications in biotechnology. *Enzyme Microb Technol* **25**, 161–171 (1999).

98. Schwan, H. P. Electrical Properties of Tissue and Cell Suspensions. in 147–209 (1957). doi:10.1016/B978-1-4832-3111-2.50008-0.

99. Cannizzaro, C., Gügerli, R., Marison, I. & von Stockar, U. On-line biomass monitoring of CHO perfusion culture with scanning dielectric spectroscopy. *Biotechnol Bioeng* **84**, 597–610 (2003).

100. Guan, Y., Evans, P. M. & Kemp, R. B. Specific heat flow rate: An on-line monitor and potential control variable of specific metabolic rate in animal cell culture that combines microcalorimetry with dielectric spectroscopy. *Biotechnol Bioeng* **58**, 464–477 (1998).

101. Arnold, S. A., Gaensakoo, R., Harvey, L. M. & McNeil, B. Use of at-line andin-situ near-infrared spectroscopy to monitor biomass in an industrial fed-batchEscherichia coli process. *Biotechnol Bioeng* **80**, 405–413 (2002).

102. Tamburini, E., Vaccari, G., Tosi, S. & Trilli, A. Near-Infrared Spectroscopy: A Tool for Monitoring Submerged Fermentation Processes Using an Immersion Optical-Fiber Probe. *Appl Spectrosc* **57**, 132–138 (2003).

103. Stärk, E. *et al.* In-Situ-Fluorescence-Probes: A Useful Tool for Non-invasive Bioprocess Monitoring. in 21–38 (2002). doi:10.1007/3-540-45736-4_2.

104. Stärk, E. *et al.* In-Situ-Fluorescence-Probes: A Useful Tool for Non-invasive Bioprocess Monitoring. in 21–38 (2002). doi:10.1007/3-540-45736-4_2.

105. Haack, M. B., Eliasson, A. & Olsson, L. On-line cell mass monitoring of Saccharomyces cerevisiae cultivations by multi-wavelength fluorescence. *J Biotechnol* **114**, 199–208 (2004).

106. Boehl, D. Chemometric modelling with two-dimensional fluorescence data for Claviceps purpurea bioprocess characterization. *J Biotechnol* **105**, 179–188 (2003).

107. Wang, F.-S., Lee, W.-C. & Chang, L.-L. On-line state estimation of biomass based on acid production in Zymomonas mobilis cultures. *Bioprocess Engineering* **18**, 329–333 (1998).

108. Hoffmann, F., Schmidt, M. & Rinas, U. Simple technique for simultaneous on-line estimation of biomass and acetate from base consumption and conductivity measurements in high-cell density cultures ofEscherichia coli. *Biotechnol Bioeng* **70**, 358–361 (2000).

109. Acuña, G., Latrille, E., Béal, C., Corrieu, G. & Chéruy, A. On-line estimation of biological variables during pH controlled lactic acid fermentations. *Biotechnol Bioeng* **44**, 1168–1176 (1994).

110. Benfer, R., Onken, U. & Werner, U. Prozeßkontrolle in der Biotechnologie mit einem On-line-Viskosimeter am Beispiel der Xanthan-Fermentation. *Chemie Ingenieur Technik* **63**, 1004–1005 (1991).

111. Marison, I. & von Stockar, U. A calorimetric investigation of the aerobic cultivation of Kluyveromyces fragilis on various substrates. *Enzyme Microb Technol* **9**, 33–43 (1987).

112. Larsson, C., Blomberg, A. & Gustafson, L. Use of microcalorimetric monitoring in establishing continuous energy balances and in continuous determinations of substrate and product concentrations of batch-grownSaccharomyces cerevisiae. *Biotechnol Bioeng* **38**, 447–458 (1991).

113. Kemp, R. B. The application of heat conduction microcalorimetry to study the metabolism and pharmaceutical modulation of cultured mammalian cells. *Thermochim Acta* **380**, 229–244 (2001).

114. Greer, C. W., Beaumier, D. & Samson, R. Application of on-line sensors during growth of the dichloroethane degrading bacterium, Xanthobacter autotrophicus. *J Biotechnol* **12**, 261–274 (1989).

115. Vallino, J. J. & Stephanopoulos, G. N. Intelligent Sensors in Biotechnology. *Ann N Y Acad Sci* **506**, 415–430 (1987).

116. Sánchez, A., Angels Gordillo, M., Montesinos, J., Valero, F. & Lafuente, J. On-line determination of the total lipolytic activity in a four-phase system using a lipase adsorption law. *J Biosci Bioeng* **87**, 500–506 (1999).

117. Desgranges, C., Georges, M., Vergoignan, C. & Durand, A. Biomass estimation in solid state fermentation II. On-line measurements. *Appl Microbiol Biotechnol* **35**, (1991).

118. Claes, J. E. & van Impe, J. F. Combining yield coefficients and exit-gas analysis for monitoring of the baker's yeast fed-batch fermentation. *Bioprocess Engineering* **22**, 195–200 (2000).

119. Boon, M., Luyben, K. Ch. A. M. & Heijnen, J. J. The use of on-line off-gas analyses and stoichiometry in the bio-oxidation kinetics of sulphide minerals. *Hydrometallurgy* **48**, 1–26 (1998).

120. Ducommun, P., Ruffieux, P.-A., Furter, M.-P., Marison, I. & von Stockar, U. A new method for on-line measurement of the volumetric oxygen uptake rate in membrane aerated animal cell cultures. *J Biotechnol* **78**, 139–147 (2000).

121. Ramirez, O. T. & Mutharasan, R. Cell cycle- and growth phase-dependent variations in size distribution, antibody productivity, and oxygen demand in hybridoma cultures. *Biotechnol Bioeng* **36**, 839–848 (1990).

122. Deshpande, R. R. & Heinzle, E. On-line oxygen uptake rate and culture viability measurement of animal cell culture using microplates with integrated oxygen sensors. *Biotechnol Lett* **26**, 763–767 (2004).

123. Oeggerli, A., Eyer, K. & Heinzle, E. On-line gas analysis in animal cell cultivation: I. Control of dissolved oxygen and pH. *Biotechnol Bioeng* **45**, 42–53 (1995).

124. Frahm, B. *et al.* Determination of dissolved CO2 concentration and CO2 production rate of mammalian cell suspension culture based on off-gas measurement. *J Biotechnol* **99**, 133–148 (2002).

125. Behrendt, U., Koch, S., Gooch, D. D., Steegmans, U. & Comer, M. J. Mass spectrometry: A tool for on-line monitoring of animal cell cultures. *Cytotechnology* **14**, 157–165 (1994).

126. Aehle, M., Kuprijanov, A., Schaepe, S., Simutis, R. & Lübbert, A. Simplified off-gas analyses in animal cell cultures for process monitoring and control purposes. *Biotechnol Lett* **33**, 2103–2110 (2011).

127. Kuprijanov, A., Schaepe, S., Aehle, M., Simutis, R. & Lübbert, A. Improving cultivation processes for recombinant protein production. *Bioprocess Biosyst Eng* **35**, 333–340 (2012).

128. Deshpande, R. R. & Heinzle, E. *On-line oxygen uptake rate and culture viability measurement of animal cell culture using microplates with integrated oxygen sensors*. *Biotechnology Letters* vol. 26 (2004).

129. Pappenreiter, M., Sissolak, B., Sommeregger, W. & Striedner, G. Oxygen uptake rate soft-sensing via dynamic kl a computation: Cell volume and metabolic transition prediction in mammalian bioprocesses. *Front Bioeng Biotechnol* **7**, (2019).

130. Villadsen, J., Nielsen, J. & Lidén, G. Gas–Liquid Mass Transfer. in *Bioreaction Engineering Principles* 459–496 (Springer US, 2011). doi:10.1007/978-1-4419-9688-6_10.

131. Garcia-Ochoa, F. & Gomez, E. Bioreactor scale-up and oxygen transfer rate in microbial processes: An overview. *Biotechnol Adv* **27**, 153–176 (2009).

132. Sieblist, C., Jenzsch, M. & Pohlscheidt, M. Influence of pluronic F68 on oxygen mass transfer. *Biotechnol Prog* **29**, 1278–1288 (2013).

133. Quijano, G., Revah, S., Gutiérrez-Rojas, M., Flores-Cotera, L. B. & Thalasso, F. Oxygen transfer in three-phase airlift and stirred tank reactors using silicone oil as transfer vector. *Process Biochemistry* **44**, 619–624 (2009).

134. Vandu, C. O. & Krishna, R. Volumetric mass transfer coefficients in slurry bubble columns operating in the churn-turbulent flow regime. *Chemical Engineering and Processing: Process Intensification* **43**, 987–995 (2004).

135. Bandyopadhyay, B., Humphrey, A. E. & Taguchi, H. Dynamic measurement of the volumetric oxygen transfer coefficient in fermentation systems. *Biotechnol Bioeng* **9**, 533–544 (1967).

136. *VB.NET - Objektorientiertes Programmieren in BV - Einstieg in die .NET Klassenbibliothek*. (2002).

137. Kühnel Andreas. *VB.NET - Objektorientiertes Programmieren in BV - Einstieg in die .NET Klassenbibliothek*. (Galileo Press GmbH, 2002).

138. Liste-Calleja, L., Lecina, M. & Cairó, J. J. HEK293 cell culture media study: increasing cell density for different bioprocess applications. *BMC Proc* **7**, P51 (2013).

139. Arena, T. A., Chou, B., Harms, P. D. & Wong, A. W. An anti-apoptotic HEK293 cell line provides a robust and high titer platform for transient protein expression in bioreactors. *MAbs* **11**, 977–986 (2019).

140. Garcia-Briones, M. A. & Chalmers, J. J. Flow parameters associated with hydrodynamic cell injury. *Biotechnol Bioeng* **44**, 1089–1098 (1994).

141. Zhan, C. *et al.* Low Shear Stress Increases Recombinant Protein Production and High Shear Stress Increases Apoptosis in Human Cells. *iScience* **23**, 101653 (2020).

142. Schwarz, H. *et al.* Small-scale bioreactor supports high density HEK293 cell perfusion culture for the production of recombinant Erythropoietin. *J Biotechnol* **309**, 44–52 (2020).

143. Sandoval-Basurto, E. A., Gosset, G., Bolívar, F. & Ramírez, O. T. Culture of Escherichia coli under dissolved oxygen gradients simulated in a two-compartment scale-down system: Metabolic response and production of recombinant protein. *Biotechnol Bioeng* **89**, 453–463 (2005).

144. Lorantfy, B., Jazini, M. & Herwig, C. Investigation of the physiological response to oxygen limited process conditions of Pichia pastoris Mut+ strain using a two-compartment scale-down system. *J Biosci Bioeng* **116**, 371–379 (2013).

145. Lara, A. R. *et al.* Transcriptional and metabolic response of recombinantEscherichia coli to spatial dissolved oxygen tension gradients simulated in a scale-down system. *Biotechnol Bioeng* **93**, 372–385 (2006).

146. Maclagan, N. F. Significance of Flocculation Tests. *BMJ* **2**, 892–896 (1948).

147. Wagner, B. A., Venkataraman, S. & Buettner, G. R. The rate of oxygen utilization by cells. *Free Radic Biol Med* **51**, 700–712 (2011).

148. Koppenol, W. H. & Butler, J. Energetics of interconversion reactions of oxyradicals. *Advances in Free Radical Biology & Medicine* **1**, 91–131 (1985).

149. Place, T. L., Domann, F. E. & Case, A. J. Limitations of oxygen delivery to cells in culture: An underappreciated problem in basic and translational research. *Free Radic Biol Med* **113**, 311–322 (2017).

150. García-Ochoa, F., Castro, E. G. & Santos, V. E. Oxygen transfer and uptake rates during xanthan gum production. *Enzyme Microb Technol* **27**, 680–690 (2000).

151. Garcia-Ochoa, F., Gomez, E., Santos, V. E. & Merchuk, J. C. Oxygen uptake rate in microbial processes: An overview. *Biochem Eng J* **49**, 289–307 (2010).

152. Ducommun, P., Ruffieux, P.-A., Furter, M.-P., Marison, I. & von Stockar, U. A new method for on-line measurement of the volumetric oxygen uptake rate in membrane aerated animal cell cultures. *J Biotechnol* **78**, 139–147 (2000).

153. Maschke, R. W., Seidel, S., Bley, T., Eibl, R. & Eibl, D. Determination of culture design spaces in shaken disposable cultivation systems for CHO suspension cell cultures. *Biochem Eng J* **177**, 108224 (2022).

154. Hofmeyr, J.-H. S. & Cornish-Bowden, A. Regulating the cellular economy of supply and demand. *FEBS Lett* **476**, 47–51 (2000).

155. Russell, J. B. & Cook, G. M. Energetics of bacterial growth: balance of anabolic and catabolic reactions. *Microbiol Rev* **59**, 48–62 (1995).

156. Ramirez, O. T. & Mutharasan, R. Cell cycle- and growth phase-dependent variations in size distribution, antibody productivity, and oxygen demand in hybridoma cultures. *Biotechnol Bioeng* **36**, 839–848 (1990).

157. Wong, T. K. K., Nielsen, L. K., Greenfield, P. F. & Reid, S. Relationship between oxygen uptake rate and time of infection of Sf9 insect cells infected with a recombinant baculovirus. *Cytotechnology* **15**, 157–167 (1994).

Appendix A CHO fermentation processes and soft sensor

Off-line determined cell concentration determinations of CHO fermentations

			Vessel 1		
date		inoculation time [h]	TCC [10^6 cells/mL]	viability [%]	VCC [10^6 cells/mL]
12.04.22	15:03	2.9	0.733	98.5	0.722
12.04.22	18:01	5.9	0.803	97.1	0.780
13.04.22	09:04	20.9	1.250	98.1	1.226
13.04.22	11:56	23.8	1.710	98.2	1.679
13.04.22	14:56	26.9	1.730	98.6	1.706
14.04.22	09:07	45.0	3.630	98.2	3.565
14.04.22	11:56	47.8	4.380	98.7	4.323
14.04.22	14:56	50.8	4.570	98.8	4.515
15.04.22	08:54	68.7	8.050	98.2	7.905
15.04.22	14:32	74.4	9.090	98.5	8.954
16.04.22	08:19	116.2	12.100	98.3	11.894
17.04.22	13:50	121.3	13.000	93.8	12.194
18.04.22	09:54	165.7	13.600	91.1	12.390
19.04.22	12:32	168.4	11.500	55.1	6.337

			Vessel 2 with script application		
date		inoculation time [h]	TCC [10^6 cells/mL]	viability [%]	VCC [10^6 cells/mL]
12.04.22	15:03	2.9	0.733	97.8	0.640
12.04.22	18:01	5.9	0.803	94.7	0.683
13.04.22	09:04	20.9	1.250	96.2	1.150
13.04.22	11:56	23.8	1.710	97.6	1.510
13.04.22	14:56	26.9	1.730	99.3	1.430
14.04.22	09:07	45.0	3.630	97.9	3.100
14.04.22	11:56	47.8	4.380	98.8	3.410
14.04.22	14:56	50.8	4.570	98.8	3.690
15.04.22	08:54	68.7	8.050	98	6.950
15.04.22	14:32	74.4	9.090	98.5	7.730
16.04.22	08:19	116.2	12.100	98.5	11.300
17.04.22	13:50	121.3	13.000	97.6	12.800
18.04.22	09:54	165.7	13.600	95.4	14.900
19.04.22	12:32	168.4	11.500	76.3	13.1

date		inoculation time [h]	Vessel 3 TCC [10^6 cells/mL]	viability [%]	VCC [10^6 cells/mL]
12.04.22	15:03	2.9	0.564	96.9	0.546516
12.04.22	18:01	5.9	0.704	95	0.6688
13.04.22	09:04	20.9	1.14	96.8	1.10352
13.04.22	11:56	23.8	1.52	98.9	1.50328
13.04.22	14:56	26.9	1.43	99.3	1.41999
14.04.22	09:07	45.0	3.18	98.3	3.12594
14.04.22	11:56	47.8	3.57	98.2	3.50574
14.04.22	14:56	50.769	3.590	98.300	3.529
15.04.22	08:54	68.738	6.900	98.000	6.762
15.04.22	14:32	74.366	7.490	98.500	7.378
16.04.22	08:19	116.158	12.200	98.800	12.054
17.04.22	13:50	121.341	9.240	96.900	8.954
18.04.22	09:54	165.741	10.600	90.300	9.572
19.04.22	12:32	168.4	9.3	40.5	3.7665

date		inoculation time [h]	Vessel 4 with script application total cell density [10^6 cells/mL]	viability [%]	VCC [10^6 cells/mL]
12.04.22	15:03	2.9	0.717	96.9	0.695
12.04.22	18:01	5.9	0.728	95	0.692
13.04.22	09:04	20.9	1.27	96.8	1.229
13.04.22	11:56	23.8	1.51	98.9	1.493
13.04.22	14:56	26.9	1.68	99.3	1.668
14.04.22	09:07	45.0	3.72	98.3	3.657
14.04.22	11:56	47.8	4.38	98.2	4.301
14.04.22	14:56	50.8	4.49	98.3	4.414
15.04.22	08:54	68.7	8.31	98	8.144
15.04.22	14:32	74.4	8.09	98.5	7.969
16.04.22	08:19	116.2	12	98.8	11.856
17.04.22	13:50	121.3	11.7	96.9	11.337
18.04.22	09:54	165.7	10.7	90.3	9.662
19.04.22	12:32	168.4	10.2	40.5	4.131

date		inoculation time [h]	Vessel 1 total cell density [10^6 cells/mL]	viability [%]	VCC [10^6 cells/mL]
03.05.22	15:25	2.9	0.811	97.7	0.792
04.05.22	09:24	20.8	1.54	98.2	1.512
04.05.22	15:41	27.1	1.83	98.7	1.806
05.05.22	09:25	44.9	3.73	98.7	3.682
05.05.22	12:25	47.9	4.03	98.6	3.974
05.05.22	15:26	50.9	4.5	98.6	4.437
06.05.22	09:42	69.1	8.04	98.4	7.911
06.05.22	12:23	71.8	8.78	98.7	8.666
06.05.22	15:08	74.6	8.64	98.7	8.528
07.05.22	11:00	94.4	11.4	98.3	11.206
07.05.22	17:44	101.2	11	98.5	10.835
08.05.22	16:52	124.3	10.8	96.3	10.400
09.05.22	10:20	141.8	11.1	90.8	10.079
09.05.22	13:32	144.0	10.6	98.1	10.399
10.05.22	13:49	168.1	10.7	56.7	

date		inoculation time [h]	Vessel 4 with script application total cell density [10^6 cells/mL]	viability [%]	VCC [10^6 cells/mL]
12.04.22	15:03	2.9	0.485	98.2	0.476
12.04.22	18:01	5.9	1.12	98.3	1.101
13.04.22	09:04	20.9	1.44	97.3	1.401
13.04.22	11:56	23.8	2.79	97.8	2.729
13.04.22	14:56	26.9	3.31	98.5	3.260
14.04.22	09:07	45.0	3.54	98.3	3.480
14.04.22	11:56	47.8	6.04	97.7	5.901
14.04.22	14:56	50.8	7.24	98	7.095
15.04.22	08:54	68.7	7.36	98.4	7.242
15.04.22	14:32	74.4	11	97.7	10.747
16.04.22	08:19	116.2	10.8	98.3	10.616
17.04.22	13:50	121.3	10.3	96.8	9.970
18.04.22	09:54	165.7	10.2	92.5	9.435
19.04.22	12:32	168.4	9.97	92	9.172
10.05.22	13:49	169.2	9.78	61.7	6.034

Data sets of dynamic OUR, VCC and qO_2 of CHO fermentations

inoculation runtime [h]	time median Script	total cell concentration [10^6 cells/mL]	viability [%]	viable cell concentration [10^6 cells/mL]	%DO consumption/h	dynamic OUR [mol/h]	dynamic OUR [mol/s]	qO_2 [mol O_2/h*cell]	qO_2 [amol O_2/s*cell]
2.9	3.2	0.64	97.8	0.626	28.59	2.00E-05	5.55E-09	1.48E-17	14.77
5.9	5.8	0.683	94.7	0.647	25.81	1.80E-05	5.01E-09	1.29E-17	12.90
20.9	20.9	1.15	96.2	1.106	59.23	4.14E-05	1.15E-08	1.73E-17	17.31
23.8	23.9	1.51	97.6	1.474	58.88	4.11E-05	1.14E-08	1.29E-17	12.92
26.9	26.9	1.43	99.3	1.420	68.83	4.81E-05	1.34E-08	1.57E-17	15.67
45.0	44.9	3.1	97.9	3.035	148.99	1.04E-04	2.89E-08	1.59E-17	15.87
47.8	47.9	3.41	98.8	3.369	173.59	1.21E-04	3.37E-08	1.67E-17	16.66
50.8	50.9	3.69	98.8	3.646	189.96	1.33E-04	3.69E-08	1.68E-17	16.85
68.7	68.7	6.95	98	6.811	289.89	2.02E-04	5.62E-08	1.38E-17	13.76
74.4	74.6	7.73	98.5	7.614	417.62	2.92E-04	8.10E-08	1.77E-17	17.73
116.2	92.2	11.3	98.5	11.131	457.44	3.19E-04	8.87E-08	1.33E-17	13.29
121.3	121.4	12.8	97.6	12.493	367.79	2.57E-04	7.14E-08	9.52E-18	9.52
165.7	141.9	14.9	95.4	14.215	388.64	2.71E-04	7.54E-08	8.84E-18	8.84
168.4	168.4	13.1	76.3	9.995	316.72	2.21E-04	6.14E-08	1.02E-17	10.25
2.9	3.2	0.717	97.7	0.701	28.17	1.97E-05	5.46E-09	1.30E-17	13.00
5.9	5.9	0.728	97.4	0.709	26.60	1.86E-05	5.16E-09	1.21E-17	12.13
20.9	20.9	1.27	98.3	1.248	66.67	4.66E-05	1.29E-08	1.73E-17	17.27
23.8	23.9	1.51	99.1	1.496	76.90	5.37E-05	1.49E-08	1.66E-17	16.62
26.9	26.9	1.68	98.6	1.656	77.49	5.41E-05	1.50E-08	1.51E-17	15.13
45.0	44.9	3.72	99	3.683	159.72	1.12E-04	3.10E-08	1.40E-17	14.02
47.8	47.8	4.38	99	4.336	166.10	1.16E-04	3.22E-08	1.24E-17	12.39
50.8	50.8	4.49	98.7	4.432	188.06	1.31E-04	3.65E-08	1.37E-17	13.72
68.7	68.7	8.31	98.7	8.202	291.49	2.04E-04	5.65E-08	1.15E-17	11.49
74.4	74.6	8.09	98.7	7.985	346.87	2.42E-04	6.73E-08	1.40E-17	14.05
116.2	92.0	12	98.9	11.868	391.47	2.73E-04	7.59E-08	1.07E-17	10.67
121.3	121.3	11.7	97.1	11.361	360.44	2.52E-04	6.99E-08	1.03E-17	10.26
165.7	141.8	10.7	92.2	9.865	333.75	2.33E-04	6.47E-08	1.09E-17	10.94
2.9	2.9	0.485	98.2	0.476	21.29	1.49E-05	4.13E-09	1.45E-17	14.45
20.8	20.9	1.12	98.3	1.101	39.06	2.73E-05	7.58E-09	1.15E-17	11.47
27.1	26.9	1.44	97.3	1.401	75.25	5.26E-05	1.46E-08	1.74E-17	17.36
44.9	44.9	2.79	97.8	2.729	161.36	1.13E-04	3.13E-08	1.91E-17	19.12
47.9	47.9	3.31	98.5	3.260	182.43	1.27E-04	3.54E-08	1.81E-17	18.09
50.9	50.9	3.54	98.3	3.480	171.54	1.20E-04	3.33E-08	1.59E-17	15.94
69.1	68.7	6.04	97.7	5.901	294.72	2.06E-04	5.72E-08	1.61E-17	16.15
71.8	71.7	7.24	98	7.095	368.66	2.57E-04	7.15E-08	1.68E-17	16.80
74.6	74.6	7.36	98.4	7.242	347.59	2.43E-04	6.74E-08	1.55E-17	15.52
94.4	95.1	11	97.7	10.747	413.44	2.89E-04	8.02E-08	1.24E-17	12.44
101.2	101.0	10.8	98.3	10.616	420.11	2.93E-04	8.15E-08	1.28E-17	12.79
124.3	124.4	10.3	96.8	9.970	397.80	2.78E-04	7.72E-08	1.29E-17	12.90
141.8	142.0	10.2	92.5	9.435	357.37	2.50E-04	6.93E-08	1.22E-17	12.25
144.0	144.9	9.97	92	9.172	344.26	2.40E-04	6.68E-08	1.21E-17	12.14

Source code for R Studio model development

```
library(readxl)
Ferm <- read_excel("Studium/Master/_Masterarbeit/CHO Soft-Sensor.xlsx")
View(Ferm)
Ferm$Vessel <- as.factor(Ferm$Vessel)
str(Ferm$Vessel)
head(Ferm)
df<-Ferm[,c(1,6,9)]
df
names(df) <- c("vsl", "cells", "o2")
names(df)
df1 <- df[-c(28,43),]
labs = colnames(Ferm[,c(1,6,9)])
if (!require('ggplot2')) install.packages('ggplot2');
library('ggplot2')

F1 <- subset(Ferm, Ferm$Vessel == "F1")
F1 <- F1[,c(1,6,9)]
names(F1) <- names(df)

ggplot(data = F1, mapping = aes(o2, cells))+
  geom_point()+
  geom_smooth(method = "gam")+
  theme_classic()

gr1<-ggplot(data = df1, aes(x = o2, y = cells))+
  geom_point()+
  geom_smooth(method = "lm", formula = y ~ x)+
  labs(
    x = "dynamic OUR [mol O2 / s]",
    y = "VCC [10^6 cells / mL]")+
  scale_y_continuous(breaks = seq(0, 14, 2))+
  scale_x_continuous(breaks = seq(0, 8e-08, 2e-08))+
  theme_classic()+
  theme(text = element_text(size = 24), aspect.ratio = 1)
 gr1
mod2 <- lm(cells ~ o2, data = df1)
summary(mod2)
plot(mod2)

df2 <- subset(df1, df1$cells<8)
summary(df2)
gr2 <- ggplot(data = df2, aes(x = o2, y = cells))+
  geom_point()+
  geom_smooth(method = "lm", formula = y ~ x)+
  labs(
    x = "dynamic OUR [mol O2 / s]",
    y = "VCC [10^6 cells / mL]")+
  scale_y_continuous(breaks = seq(0, 10, 1))+
  scale_x_continuous(breaks = seq(0, 14e-08, 2e-08))+
  theme_classic()+
  theme(text = element_text(size = 24), aspect.ratio = 1)
gr2
mod1 <- lm(cells ~ o2, data = df2)
summary(mod1)
plot(mod1)
```

Output from R Studio

```
Call:
lm(formula = cells ~ o2, data = df1)

Residuals:
    Min      1Q  Median      3Q     Max
-3.2794 -0.6992 -0.0324  0.4335  4.1119
Coefficients:
              Estimate Std. Error t value Pr(>|t|)
(Intercept) -5.015e-01  3.874e-01  -1.295    0.203
o2           1.406e+08  7.569e+06  18.581   <2e-16 ***
---
Signif. codes:  0 ‘***’ 0.001 ‘**’ 0.01 ‘*’ 0.05 ‘.’ 0.1 ‘ ’ 1

Residual standard error: 1.341 on 39 degrees of freedom
Multiple R-squared:  0.8985,Adjusted R-squared:  0.8959
F-statistic: 345.3 on 1 and 39 DF,  p-value: < 2.2e-16

Call:
lm(formula = cells ~ o2, data = df2)

Residuals:
    Min      1Q  Median      3Q     Max
-0.8940 -0.2042 -0.0636  0.1529  0.9001
Coefficients:
             Estimate Std. Error t value Pr(>|t|)
(Intercept) 1.064e-01  1.344e-01   0.792    0.436
o2          1.037e+08  3.618e+06  28.662   <2e-16 ***
---
Signif. codes:  0 ‘***’ 0.001 ‘**’ 0.01 ‘*’ 0.05 ‘.’ 0.1 ‘ ’ 1

Residual standard error: 0.4319 on 26 degrees of freedom
Multiple R-squared:  0.9693,Adjusted R-squared:  0.9681
F-statistic: 821.5 on 1 and 26 DF,  p-value: < 2.2e-16
```

Appendix B HEK fermentation processes

Off-line determined cell concentration determinations of HEK fermentations

			Vessel 1		
date		inoculation time [h]	TCC [10^6 cells/mL]	viability [%]	VCC [10^6 cells/mL]
02.02.22	13:40	20.83	0.342	97.4	0.333
03.02.22	10:00	41.4	0.185	94.2	0.174
04.02.22	10:00	65.4	0.138	92	0.127
05.02.22	10:40	89.4	0.0937	77.6	0.073
06.02.22	14:15	110.3	0.096	90.8	0.087

			Vessel 2		
date		inoculation time [h]	TCC [10^6 cells/mL]	viability [%]	VCC [10^6 cells/mL]
02.Feb	13:40	20.83	0.332	97.7	0.324
03.Feb	10:00	41.4	0.321	94.2	0.302
04.Feb	10:00	65.4	0.272	90.3	0.246
05.Feb	10:40	89.4	0.0529	87.5	0.046
06.Feb	14:15	110.3	0.0176	62.5	0.011

			Vessel 3		
date		inoculation time [h]	TCC [10^6 cells/mL]	viability [%]	VCC [10^6 cells/mL]
02.Feb	13:40	20.83	0.173	94.3	0.163
03.Feb	10:00	41.4	0.178	90.1	0.160
04.Feb	10:00	65.4	0.184	93.4	0.172
05.Feb	10:40	89.4	0.133	85.1	0.113
06.Feb	14:15	110.3	0.11	87	0.096

			Vessel 4		
date		inoculation time [h]	TCC [10^6 cells/mL]	viability [%]	VCC [10^6 cells/mL]
02.Feb	13:40	20.50	0.587	97.6	0.573
03.Feb	10:00	41.1	0.664	95.2	0.632
04.Feb	10:00	65.1	0.730	95.0	0.694
05.Feb	10:40	90.0	1.06	94.9	1.006
06.Feb	14:15	117.2	1.29	91.4	1.179
07.Feb	14:11	136.7	1.85	89	1.647
08.Feb	14:12	161.5	3.03	85.2	2.582
09.Feb	14:11	185.2	3.6	76.9	2.768

			Vessel 1 with script application		
date		inoculation time [h]	TCC [10^6 cells/mL]	viability [%]	VCC [10^6 cells/mL]
03.Mär	15:15	2.00	0.453	94.6	0.429
04.Mär	09:00	20.1	0.347	92.7	0.322
04.Mär	15:00	25.7	0.396	97.5	0.386
05.Mär	14:50	51.9	0.285	90.3	0.257
06.Mär	15:05	71.9	0.319	91.7	0.293
07.Mär	10:05	90.9	0.244	93.2	0.227

			Vessel 2 with script application		
date		inoculation time [h]	TCC [10^6 cells/mL]	viability [%]	VCC [10^6 cells/mL]
03.Mär	15:15	2.00	0.571	98.5	0.562
04.Mär	09:00	20.1	0.549	95.2	0.523
04.Mär	15:00	25.7	0.473	95.8	0.453
05.Mär	14:50	51.9	0.641	93.3	0.598
06.Mär	15:05	71.9	0.495	95.8	0.474
07.Mär	10:05	90.9	0.645	93	

			Vessel 3		
date		inoculation time [h]	TCC [10^6 cells/mL]	viability [%]	VCC [10^6 cells/mL]
03.Mär	15:15	2.00	0.612	96.9	0.593
04.Mär	09:00	20.1	0.673	96.6	0.650
04.Mär	15:00	25.7	0.544	95.7	0.521
05.Mär	14:50	51.9	0.651	94.6	0.616
06.Mär	15:05	71.9	0.71	93.6	0.665
07.Mär	10:05	90.9	0.954	90.8	

			Vessel 4 with script application		
date		inoculation time [h]	TCC [10^6 cells/mL]	viability [%]	VCC [10^6 cells/mL]
03.Mär	15:15	2.00	0.614	96.9	0.595
04.Mär	09:00	20.1	0.708	95.6	0.677
04.Mär	15:00	25.7	0.687	95.7	0.657
05.Mär	14:50	51.9	0.886	93.9	0.832
06.Mär	15:05	71.9	1.01	94.4	0.953
07.Mär	10:05	90.9	0.856	92.8	0.794

Appendix C Tn*ms*42 processes

Off-line determined cell concentration determinations of Tn*ms*42 fermentations

			Vessel 1		
date		inoculation time [h]	TCC [10^6 cells/mL]	viability [%]	VCC [10^6 cells/mL]
15.06.22	11:45	0.3	0.833	90.6	0.754698
16.06.22	14:17	2.9	0.728	92	0.66976
17.06.22	11:23	24.0	1.77	94.6	1.67442
18.06.22	17:18	29.9	2.06	94.7	1.95082
19.06.22	08:31	45.1	3.51	94.5	3.31695
20.06.22	11:16	47.9	4.51	95.2	4.29352
21.06.22	17:18	53.9	5.26	95.7	5.03382
22.06.22	17:27	78.0	8.66	96	8.3136
23.06.22	11:23	96.0	8.63	93.2	8.04316

			Vessel 3 with script application		
date		inoculation time [h]	TCC [10^6 cells/mL]	viability [%]	VCC [10^6 cells/mL]
15.06.22	11:45	0.3	0.872	89.9	0.784
16.06.22	14:17	2.9	0.871	92.8	0.808
17.06.22	11:23	24.0	2.03	95.2	1.933
18.06.22	17:18	29.9	2.5	94.8	2.370
19.06.22	08:31	45.1	4.3	95.8	4.119
20.06.22	11:16	47.9	5.11	95.9	4.900
21.06.22	17:18	53.9	6.52	95.3	6.214
22.06.22	17:27	78.0	9.36	95.4	8.929
23.06.22	11:23	96.0	9.29	88.9	8.259

			Vessel 4 with script applicaiton		
date		inoculation time [h]	TCC [10^6 cells/mL]	viability [%]	VCC [10^6 cells/mL]
15.06.22	11:45	0.3	0.753	91.8	0.753
16.06.22	14:17	2.9	0.819	86.4	0.819
17.06.22	11:23	24.0	1.880	95	1.880
18.06.22	17:18	29.9	2.210	94.3	2.210
19.06.22	08:31	45.1	4.120	93.4	4.120
20.06.22	11:16	47.9	4.630	94.2	4.630
21.06.22	17:18	53.9	5.440	93.5	5.440
22.06.22	17:27	78.0	10.600	93.7	10.600
23.06.22	11:23	96.0	10.500	91.1	9.566

			Vessel 3		
date		inoculation time [h]	TCC [10^6 cells/mL]	viability [%]	VCC [10^6 cells/mL]
28.06.	12:07	0.26	0.504	92.8	0.468
28.06.	14:46	2.90	0.54	91.6	0.495
29.06.	08:55	21.06	1.19	95.3	1.134
29.06.	14:42	26.83	1.36	93.7	1.274

date	inoculation time [h]	Vessel 4 with script applicaiton		
		TCC [10^6 cells/mL]	viability [%]	VCC [10^6 cells/mL]
28.06. 12:07	0.26	0.595	93.7	0.558
28.06. 14:46	2.90	0.571	88.8	0.507
29.06. 08:55	21.06	1.11	95	1.055
29.06. 14:42	26.83	1.33	93.3	1.241

Data sets of dynamic OUR, VCC and qO_2 of Tn*ms*42 fermentations

inoculation runtime [h]	viable cell density [Mio cells/mL]	%DO consumption/h	dynamic OUR [mol/h]	dynamic OUR [mol/s]	qO2 [mol O2/s*cell]	qO2 [amol O2/s*cell]
2.9	0.808	12.40	8.66E-06	2.41E-09	4.96E-18	5.0
24.0	1.933	20.87	1.46E-05	4.05E-09	3.49E-18	3.5
29.9	2.370	1.84	1.29E-06	3.57E-10	2.51E-19	0.3
45.1	4.119	73.49	5.13E-05	1.43E-08	5.77E-18	5.8
47.9	4.900	38.21	2.67E-05	7.41E-09	2.52E-18	2.5
53.9	6.214	52.49	3.67E-05	1.02E-08	2.73E-18	2.7
78.0	8.929	26.71	1.87E-05	5.18E-09	9.67E-19	1.0
96.0	8.259	41.83	2.92E-05	8.11E-09	1.64E-18	1.6
2.9	0.708	41.49	2.90E-05	8.05E-09	1.90E-17	19.0
24.0	1.786	27.85	1.94E-05	5.40E-09	5.04E-18	5.0
29.9	2.084	143.53	1.00E-04	2.78E-08	2.23E-17	22.3
45.1	3.848	69.12	4.83E-05	1.34E-08	5.81E-18	5.8
47.9	4.361	77.89	5.44E-05	1.51E-08	5.77E-18	5.8
53.9	5.086	97.30	6.80E-05	1.89E-08	6.18E-18	6.2